1973

An electron paramagnetic resonance study of indium doped zinc oxide.

Van der Schroeff, Coenraad.

Monterey, California. Naval Postgraduate School

AN ELECTRON PARAMAGNETIC RESONANCE STUDY OF INDIUM DOPED ZINC OXIDE

Coenraad van der Schroeff

NAVAL POSTGRADUATE SCHOOL
Monterey, California

THESIS

An Electron Paramagnetic Resonance
Study of Indium Doped Zinc Oxide

by

Coenraad van der Schroeff

Thesis Advisor: William M. Tolles

June 1973

Approved for public release; distribution unlimited.

An Electron Paramagnetic Resonance Study of Indium Doped Zinc Oxide

by

Coenraad van der Schroeff
Lieutenant Commander, United States Navy
BS, Trinity College, 1964

Submitted in partial fulfillment of the requirements for the degree of

MASTER OF SCIENCE IN CHEMISTRY

from the

NAVAL POSTGRADUATE SCHOOL
June 1973

ABSTRACT

Samples of zinc oxide doped with indium have been prepared using the vapor transport method. Concentration of dopant is controlled by appropriate mixing of the oxides of indium and zinc.

When ZnO is mechanically damaged, three lines in the EPR spectrum with g-values at 2.0052, 2.0136, 2.0184 are induced. These are attributed to the interaction of adsorbed species and induced paramagnetic centers in the crystal. The relative intensity of the lines is affected by indium doping.

Spin density measurements using first moment calculations (M*) on ZnO-In did not show a linear correlation with concentration. This is attributed to spin pairing of the electrons. The g-value for ZnO-In varied depending on concentration from 1.9563 to 1.9591, and was found to be independent of temperature and pressure.

Based on the behavior of M*T and M* for In doped ZnO the electrons giving rise to the EPR spectrum were thought to be in a shallow donor band.

TABLE OF CONTENTS

LIST OF TABLES

LIST OF ILLUSTRATIONS

INTRODUCTION

The electron paramagnetic resonance (EPR) characteristics of zinc oxide have been of interest to many investigators for a number of years. Of particular concern is the physical and chemical nature of surface species adsorbed on polycrystalline ZnO in catalyzed gaseous reactions, the effect of impurity doping on the semiconducting properties of ZnO, UV and X-ray radiation effects on stability of ZnO when used in thermal coatings, and the luminescent properties of ZnO with impurity doping.

In the majority of these studies ZnO has exhibited EPR lines in the vicinity of the free electron @ g=2.002 and others @ g=1.96. The nature of these lines has been characterized but their origin is not completely understood.

The aim of this study is to further characterize the nature of the EPR line @ g=1.96 and to present a model which explains the origin of the signal observed.

ZnO is an intrinsic semiconductor with a band gap of 3.2eV [1]. Donor or acceptor doping of ZnO is expected to change its conductivity and hence its EPR signal. Since even small amounts of acceptor doping with, for example, Li^+ reduces the ZnO EPR spectral lines below the detection limit [2] it was decided to use the donor indium as a doping agent. It was hoped that a correlation could be found between the level of doping and the EPR measured spin density of intensity of the line @ g=1.96.

Throughout the study of ZnO, polycrystalline doped and undoped samples were used with varying conditions of temperature, vacuum, and doping level. Samples were prepared by two methods: (1) sintering of a mixture of ZnO and In_2O_3 and (2) vapor phase growth of small crystals from similar mixtures which had been fashioned into cylinders for use in a tubular furnace. These will be described in the experimental section.

A general historical review of pertinent past research efforts will provide a background for evaluating the observations of this work.

HISTORICAL REVIEW

This historical review starts with the work of D. G. Thomas [3], which provided some of the fundamental observations on which later investigators draw. Thomas made a study of single crystal zinc oxide doped with indium as a donor impurity. Single crystals of the zinc oxide were prepared by vapor transport techniques, doped by painting the crystals with indium nitrate, and fired at temperatures from 900-1250°C. Conductivity, electron mobilities, and the rate of diffusion of indium into zinc oxide were determined.

The highest conductivity in these doped ZnO crystals was found to occur when the crystals had a faint blue/green color. The color was ascribed to the effect of free carrier absorption at the end of the visible spectrum. It was also found that after a certain period of time, depending upon the firing temperature and oxygen partial pressure, equilibrium with dissolved and precipitated indium in the zinc oxide crystal could be obtained, and depending upon subsequent treatment (i.e., quenching or annealing), supersaturation with indium could result. Since indium must be considered a donor impurity, the conductivity of zinc oxide should be increased by the amount of unprecipitated indium in the crystal.

Thomas [3] makes the assumption that the conductivity is proportional to the average concentration of unprecipitated

indium in the crystal. By determining the limit of solubility of indium he found that diffusion rates of indium into the crystal depended on the oxygen partial pressure with the diffusion rate increasing as the partial pressure was increased. In addition, conductivity was seen to depend upon the oxygen partial pressure. The kinetics of these changes of conductivity with oxygen partial pressure were not analyzed in detail but the changes were time dependent and were comparable to the time necessary for initial precipitation of indium once saturation had been reached. This relationship may be explained by reaction

$$(In_2O_3)\,surface \longrightarrow 2In_{zn}^{+} + 2O_o + 2e^{-} + \tfrac{1}{2}O_2$$

(where only deviations from the normal lattice point charge is indicated by the subscripts) in which it is assumed that for each interstitial indium, one free electron is obtained. With this in mind, and in applying the law of mass action to the above equation, the conductivity is inversely proportional to the eighth root of the oxygen partial pressure.

Thomas [3] also investigated the effect of additional zinc doping in the indium doped zinc oxide. Zn^{+} should act as an acceptor and thus reduce the number of free electrons available from the indium doping, thereby decreasing the crystal conductivity. This relationship was observed.

Whereas Thomas [3] did not use EPR in any part of his study, Walters et al [4] found it to be particularly suited to the study of induced paramagnetic centers in mechanically damaged Group IV semiconductors and Group II-VI compounds.

The technique may be used to determine if such defect centers are present and to what degree the surface of these materials may have been damaged. The damage process did not involve any impurities that may be present in the starting material and it was apparent that the centers were due to the damaging treatment. These conclusions were corroborated by additional studies of neutron induced radiation damage which resulted in similar paramagnetic resonance centers. When mechanically damaged, materials in the above groups showed resonance lines with g-values in the neighborhood of 2. Silicon and magnesium oxide were primarily investigated. Zinc oxide was among the compounds cursorily investigated and was found to produce a resonance line at $g \approx 2$.

Kokes [5] investigated the behavior of the line g=1.96 under varying vacuum/heat pretreatments of zinc oxide catalysts and found that depending on the conditions, two independent oxygen species may be adsorbed on the catalyst surface. The investigation was conducted using acceptor and donor doped zinc oxide (lithium, aluminum or gallium). Undoped zinc oxide at room temperature and atmospheric pressure showed only a very weak resonance line at g=1.96 but the intensity of the doped samples was markedly stronger. Kokes [5] showed that these changes are due to the doping and are the result of the added ions. According to his results,

> "...if the catalyst is treated in a manner known to increase its conductivity (irradiated at -195°C, evacuated, doped with gallium, aluminum, or adsorbed hydrogen at 210°C) the signal at g=1.96 increases; if it is treated in a manner known to decrease its conductivity (calcinated

at high temperature, or doped with lithium) the signal decreases.".

Other data show that when the evacuated catalyst is exposed to air (which decreases the conductivity) the signal decreases. Kokes thus concluded that the resonance line at g=1.96 is due to conduction electrons.

In these experiments Kokes [5] also added varying amounts of oxygen (at room temperature) on previously degassed (at high temperature) zinc oxide, and subsequent evacuation did not restore the resonance line to its full intensity. As a consequence, a large percentage of the oxygen adsorbed at room temperature was strongly held and it is this species which decreases the signal. In reference to earlier work by other researchers, Kokes [5] postulated that two oxygen species were involved; the O^- ion mainly responsible for decrease of the signal at room temperature and to a lesser extent the O^{2-} ion at high temperature. This in turn contributed to the decrease in conductivity of ZnO. The high temperature adsorption occurred at 400°C and above.

Kokes [5] computed the spin density from the observed resonance line using a first moment calculation with $CuSO_4 \cdot 5H_2O$ as a comparison standard. Since he stated

"The electron spin resonance signal has been shown to reflect changes in the number of free electrons.",

he concluded

"...there can be little doubt that the signal observed for zinc oxide at g=1.96 is due to un-ionized donors and/or conduction electrons."

and further, although it cannot be ruled out that the signal is due to un-ionized donors,

> "...the lack of splitting due to nuclear spin of gallium and aluminum for the doped samples together with the increase in the signal during ultraviolet irradiation of undoped samples are consistent with the interpretation that the signal is due to conduction electrons.".

He also showed the the O^{2-} species contributed far less than the O^{-} species to the number of free electrons available and, therefore, the adsorbed species responsible for the decrease in the electron paramagnetic resonance signal at room temperature is O^{-}.

Electron paramagnetic resonance lines in Group II-VI semiconductors and phosphors with impurity doping have g-values smaller than those for free electrons and show no hyperfine structure. Müller and Schneider [1] attributed these signals to mobile electrons in the conduction band or shallow donor bands. The wave functions of the electrons in Group II-VI compounds are essentially s-character and this holds for both conduction band and donor band electrons. It is reasoned that as the dopant concentration of donor impurities increases the indium donor band wave functions mix with the zinc oxide conduction band wave functions. At some lower concentration the onset of the overlap of donor wave functions gives rise to the donor band. It was estimated for zinc oxide that donor band and conduction band overlap occurs at concentrations of $6X10^{18}$ cm^{-1} ($\simeq 9X10^{19}$/mole). In order to verify the onset of a donor band it would be necessary to obtain zinc oxide in a purity such that donor concentration

would be less than 10^{18} cm^{-3}. It is stated that below the level of C_d (concentration at which wave function overlap begins to occur) the EPR resonance line would show hyperfine structure but that above this concentration only a single line will be observed. Müller et al [1] observed in indium doped single crystals of zinc oxide, donor concentration on the order of $5X10^{19}$ cm^{-3} with a g-value equal to 1.96. This same line has been observed in undoped samples but at much reduced intensity.

Irradiation by ultraviolet light would increase the intensity, exciting electrons from the valence into the conduction band. The lack of hyperfine structure was attributed to the electrons being in the conduction band, but in the picture of donor band and conduction band wave function overlap, it would not be required to have hyperfine structure even though the electrons were not in the conduction band itself. It was also postulated that the donor electron g-value is slightly higher than those of electrons in the conduction band. To some extent, g-values were dependent upon a particular dopant, the properties of the lattice, and treatment given during preparation. Therefore, with regard to the relative g-values and line widths, according to the Elliott (referenced therein) relaxation mechanism, the

> "...T_1 of the carrier electron spin resonance is, for identical g-values proportional to the mobilities which are higher in the conduction than in the donor band;...".

It is expected that the conduction band electron spin resonance line width would be narrower than for donor band electrons

and the g-value of conduction electrons slightly larger than the g-value of donor electrons.

Kasai [6] observed two lines at g=1.956 of which the higher g-value was attributed to halogen ions and the lower to oxygen vacancies. In these experiments Kasai prepared samples in which zinc oxide was doped with various concentrations of NaCl where behavior of the line at g=1.960, which he attributed to a halogen donor, was observed at various concentrations, spectrometer power levels, and temperatures. Since these signals (i.e., oxygen vacancies and substitutional halogen ions) occurred very close to each other it was reasoned that overlap of these signals could readily cause scattering of g-values in the region of g=1.96.

Rauber and Schneider [7] studied the effect of substitutional In^{2+} in zinc sulphide and observed strong hyperfine interaction with the nuclear spin of the impurity centers. The indium occupied substitutional zinc sites and the impurity centers were assumed to be In^{+} and In^{3+}, both of which are diamagnetic. In addition to indium, both aluminum and gallium were incorporated in different samples as donors. A comparison of the aluminum and indium doped samples revealed that whereas indium showed hyperfine structure in ZnS, none could be seen in the aluminum doped samples. The difference in behavior of aluminum and indium may be due to the fact that stable aluminum occurs only in the trivalent state whereas indium occurs as In^{+} and In^{3+}. Under these conditions, indium may also occur as charge compensated ion pairs. If an

unpaired electron were localized in the vicinity of this ion pair, hyperfine structure would be reasonable. Rauber et al [7] found it surprising, however, that in zinc oxide doped with indium only a single isotropic line was seen. This observation was attributed to an ESR line characteristic of mobile electrons.

Lunsford and Jayne [8] studied the interaction of oxygen with zinc oxide. In their experiments ZnO was degassed and then (at room temperature) exposed to O_2 from pressures of 0.5μ to 20μ. EPR spectra were obtained at -190°C. All spectra showed a characteristic triplet with g_{xx}=2.051, g_{yy}=2.0020 and g_{zz}=2.0082. The adsorbed species on this degassed ZnO could be O_3^-, O^-, O^{2-}, O_2^-, or a peroxy group. It was concluded that adsorption at low temperatures occurred as the O_2^- species (in contrast to Kokes [5]) and, since at higher temperatures free electrons are more available according to the reaction

$$O + e^- \longrightarrow O^- + 2.1eV,$$

the O^- species was adsorbed. Regardless of the assignments, oxygen adsorbs as a species with an unpaired electron and the net result is transfer of an electron from the solid to the oxygen molecule.

In a brief study of polycrystalline and single crystal ZnO, under conditions of UV irradiation, Lal et al [9] reported a signal at g=1.95392 attributed to electrons trapped at oxygen vacancies (F center). Had the signal been due to Zn^+ detectable hyperfine satellites of Zn^{67} (I=5/2 with a natural abundance of 4.1%) should be observed, but, since

only a single line was found, the resonance was not attributed to this species.

Sancier [10] studied zinc oxide and its influence as a catalyst in the oxidation of carbon monoxide. In polycrystalline samples of zinc oxide, which had been degassed at high temperatures and still under vacuum, he observed the usual line @ g=1.96. When the degassed sample was treated with small amounts of O_2 the intensity of the line decreased but subsequent reaction with CO caused the intensity of the line to be partially restored. Line broadening also occurred. This was attributed to an increase in concentration of electrons in the bulk ZnO after reaction. The conclusion was that increase in intensity was due to the reaction:

$$O^- + CO \longrightarrow CO_2 + e^- \quad \text{(to conduction band)}.$$

The reaction of CO being oxidized to CO_2 over ZnO occurred rapidly and in Sancier's work it was shown that the intensity of the signal at g=1.96 increased to some steady state value in time. This steady state value of signal intensity was correlated with a measured amount of presorbed O_2. Thus, the spin density in ZnO corresponded to the total amount of O_2 reacted and hence the number of electrons transferred from O^- species to the bulk ZnO. In addition to the line @ g=1.96 a line @ g=2.01 was also observed for incompletely outgassed ZnO. Upon reaction of CO with the surface adsorbed oxygen, the behavior of this line differed from that at g=1.96. In particular, the rate of change of intensity of the line @g=2.01 was significantly slower than for the

line@ g=1.96 requiring that the mechanism for the CO reaction on the ZnO surface proceeded by two different paths. Noting that the reaction of CO on completely outgassed ZnO produces no change in the ZnO spectrum but when oxygen is presorbed the reaction of CO to CO_2 does, different oxygen species must account for the two different lines. Based on an earlier study [8] it was postulated that the slower reacting species was O_2^- and the faster reacting was O^-. The former may or may not involve electron transfer to the bulk ZnO.

In a similar study [11] the behavior of ZnO as a catalyst used for the reduction of nitric oxide to nitrogen in air pollution control was investigated. The surface interaction of nitric oxide on zinc oxide was shown to produce the desired reduction and in this study by Lunsford [11] two species NO and NO_2^{2-} were classified with g-values for adsorbed NO ($g_{xx}=g_{yy}=1.999$ and $g_{zz}=1.94$) and for NO_2^{2-}, ($g_{xx}=g_{yy}=2.0057$, $g_{zz}=2.0026$).

Codell et al [12] studied the adsorption of t-butyl hydroperoxide (TBHP) on outgassed ZnO. After outgassing at 500°C, two signals @ g=1.965 and 1.961 appeared. For both to occur outgassing above 350°C was required. Outgassed ZnO at 500°C treated with oxygen at room temperature and re-outgassed, showed the typical spectrum of O_2^- at g=2.005 [8]. The signal which appeared in the neighborhood of g=1.96 was somewhat modified by line broadening. Under various pretreatments of ZnO (i.e., outgassing temperature, presorption oxygen treatment, etc.) the signal at g=1.96 could be resolved into two distinct signals. These signals at g=1.961

and 1.965 behaved independent of each other and at high temperature pretreatment the signal at g=1.965 decreased, at lower temperatures the signal at 1.961 decreased. These observations led to the assignment of the g=1.965 line to Zn^+ and g=1.961 to O^-. This assignment was justified by noting that according to Thomas [3] most interstitial zinc is removed at 500°C with the reaction being

$$Zn^+ + O^-(\text{from TBHP}) \longrightarrow Zn^{2+} + O^{2-},$$

and decrease of the 1.961 line according to the reaction

$$O^- + e^- \longrightarrow O^{2-}.$$

Iyengar et al [13] extensively studied the interaction of oxygen, various nitrogen oxides, and chlorine on zinc oxide. As in previous studies, ZnO outgassed at 500°C produced a strong g=1.96 line and a very weak line at g=2.003. Subsequent treatment with oxygen produced a weak 1.96 line and the line at g=2.003 became a triplet. Upon heating under vacuum, the original signal intensities were restored. Addition of excess oxygen broadened the triplet @ g=2.003 and with even more oxygen, eliminated it. The triplet was assigned to O_2^- ions formed at the surface.

Sancier [10] had suggested that this triplet may have possibly been due to a complex process of CO_2 or H_2O absorption. However, Iyengar et al [13] established that this triplet must be caused by a single species. For example, if the triplet @ g=2.003 were due partially to O_2^- and partially to O^- (i.e., two species), by increasing the temperature of the sample, the triplet would become a singlet. However,

this did not occur - the triplet simply disappeared at about 350°C.

When ZnO was treated with NO_2, the line at g=1.96 decreased and a sharp symmetrical signal at g=2.0015 appeared. However, this signal was not observed above -130°C and when excess NO_2 was removed, a complex spectrum, somewhat difficult to reproduce, resulted. This signal (g=2.0015) was attributed to adsorbed NO_2 molecules on ZnO. The spectrum resulting from outgassing showed both g and hyperfine anisotropy to be present where g_{xx}, g_{yy}, and g_{zz} were split into three lines due to interaction with the N nucleus (I=1/2). This assignment was further confirmed with N^{15} enriched NO_2. Note that no electron transfer is involved.

Treatment with N_2O resulted in a spectrum with g=1.957 and g=1.961. Heating and removal of excess N_2O (and possible reaction products) resulted in a single line with g=2.0015.

Adsorption of NO on ZnO resulted in a symmetric triplet centered at g=2.000 and a shoulder at g=2.003. The behavior of CO_2 adsorbed on ZnO was similar to that of NO_2 in that the g=1.96 line intensity decreased and a signal at g=2.0015 appeared.

Iyengar et al [13] considered the signals at g=1.957 and g=1.961 to be identical to the signals found by Codell [12] for TBHP adsorbed on ZnO and any discrepancies noted to be due to experimental error. The signals were not attributed to any particular species adsorbed from the gas phase, but were considered to be due, as suggested by Codell [12], to

the interaction of the adsorbed species with Zn^+ sites and electrons trapped in anionic vacancies:

$$N_2O + Zn^+ \longrightarrow N_2O^- + Zn^{2+},$$

and

$$N_2O + e^-(\text{vacancies}) \longrightarrow N_2O^-,$$

where the electrons are removed from the ZnO to the adsorbed species thus reducing the intensity of the signal at g=1.96.

Observation of the decrease in intensity of the line @ g=1.96 upon O_2 adsorption on outgassed ZnO led Setaka et al [14] to postulate that conductivity could be related to the change in the EPR spectrometer cavity Q. Since the adsorption of O_2 was thought to involve an electron transfer from the bulk ZnO to the sorbed O_2, the concentration of electrons in the conduction band or shallow donor band must decrease. This concept was further supported by the increase in intensity of the line @ g=2.0 which is attributed to the adsorbed species. Thus, if electrons are transferred to the sorbed species the electron density in the ZnO must decrease, causing a significant change in ZnO conductivity which, in turn, must effect the cavity Q. Using Mn^{2+} as a standard by which to qualitatively observe changes in Q, and measurement of spectrometer crystal current for quantitative values, Setaka et al [14] obtained, under varying O_2 pressure conditions, first moment electron density values.

These electrons were considered to be conduction electrons rather than donor state electrons because the observed densities were an order of magnitude greater than would be

expected if the maximum concentration of dissolved zinc in ZnO [3] were obtained. It is clear here that donor electrons are considered to be due only to dissolved zinc. The theory presented provided a direct relationship between EPR signal intensity, spectrometer crystal current, conduction band electrons, and, hence, sample conductivity. In particular, it provided a measurement of available electrons for catalysis which occurs by electron transfer from the bulk catalyst to the reacting species.

Elucidation of two signals @ g=1.96 by doping of ZnO with Al^{3+} or Li^{+} was further studied by Setaka et al [2]. The intent was to control the electron concentration with either the acceptor Li^{+} or the donor Al^{3+}. All spectra were obtained at -195°C. Doping was accomplished by slurrying ZnO with aluminum and lithium nitrate (there was no observable anion effect) and heating at 500°-700°C. Pretreatment with O_2 on vacuum outgassed ZnO resulted in decreased intensity of the line @ g=1.96 and the signal shape was not effected. At LN_2 temperatures this one line was resolved into two at g=1.963 and g=1.957. With additional O_2 pretreatment the intensity of the former decreased, the latter remained the same. Furthermore, exposure of ZnO to H_2O vapor, which is known to increase its conductivity [5], caused the line g=1.957 intensity to increase. Based on these observations, the line g=1.957 was attributed to conduction electrons in the bulk ZnO.

On the other hand, adsorption of O_2 decreased the ZnO conductivity and did not effect g=1.957. Donor doping (Al^{3+})

increased the 1.957 intensity while acceptor doping (Li^+) caused it to vanish. Setaka et al [2] conclude that electrons in the bulk ZnO are expected to be either in the conduction band or at localized donor states (i.e., interstitial Zn^+ or trapped at oxygen ion vacancies). Finally, the behavior of a line at g=2.0013 was opposite to that of the line at g=1.957, the former being attributed to possible holes in acceptor levels.

Iron cyanide provides efficient electron hole recombination centers [15] and when adsorbed on ZnO under vacuum conditions, produced a doublet in the ESR spectrum at g_1=1.9600 and g_2=1.9564. Under UV irradiation the line g_2 increased significantly and on subsequent exposure to O_2 with the UV turned off, decreased irreversibly. g_1 did not appear to be effected by such treatment. When the iron cyanide concentration was high and the O_2 pressure low, the two lines could not be resolved but, evidence of their existence was seen by slight shift in g when the sample was exposed to various low O_2 pressure conditions. These observations led Sancier [15] to suggest that both components are due to conduction electrons and the difference in g-value due to some electrons being in the vicinity of precipitated excess zinc and others being unperturbed conduction electrons. g_1 was assigned to the former condition and g_2 to the latter. The decrease in line intensity upon exposure to O_2 is caused by the removal of electrons from the conduction band by the adsorbed species.

> "The remaining spin density is associated with electrons beyond the surface space charge region in the normal conduction band (g_2) and those interacting with localized excess zinc (g_1)."

In an investigation of photoinduced processes in zinc oxide [16], a single EPR signal was observed with a g-value of @ g=1.96. In the opinion of the authors,

> "...the EPR signal is not a result of free electrons but supports the localized model of a paramagnetic centre that can act as trapping centres. The EPR intensity is given as well by the number of oxygen vacancies as by the presence and cross-sections of other trapping centres.",

these being strongly influenced by the method of preparation. In this study, the activation energy of photosensitive centers was computed (E_A=0.52±0.02) which is somewhat in agreement with a similar study [17].

In a number of previous studies it had often been commented that the exact nature of the EPR spectrum of ZnO depended on the preparation methods of the sample. With this in mind, Gerasimova et al [18] studied the dependence of the EPR signal on various preparation methods of zinc oxide. In general the preparation techniques aimed at producing zinc rich ZnO, zinc poor ZnO under vacuum and in air, and acceptor and donor doped ZnO samples. Two lines were observed which rarely occurred simultaneously and the line width was either 5 or 9 G. Those lines with ΔH=9G had g-values of 1.957 and 1.961, and were attributed to unpaired electrons from donor levels arising from oxygen vacancies and excess zinc, respectively. The line with ΔH=5G at g=1.957 was due to the

formation of narrow donor bands. Aluminum doped ZnO did not show direct proportionality in intensity with percent dopant.

In yet another study on the behavior of zinc oxide with adsorbed oxygen, Tanaka et al [19] propose two types of adsorbed oxygen species. Desorption of high temperature pre-outgassed zinc oxide exposed to 8 cm Hg of O_2 pressure resulted in two peaks in gas chromatographic analysis. A high temperature peak was attributed to O^- and the low temperature peak to O_2^-. The GC spectrum was obtained by re-evacuating ZnO after an O_2 treatment and running a temperature programmed desorption while sampling the desorbed products at specified temperature intervals. These were then analyzed on a gas chromatograph. Reactivity of the desorbed species was determined by the passage of a CO pulse over the sample and it was observed that the high temperature peak attributed to O^- disappeared completely on subsequent GC analysis. Depending on the manner in which adsorption of oxygen was allowed to occur, the peaks could be made to change in relative intensity. The high temperature peak disappearance after CO pulse passage was attributed to the reaction

$$CO + O^- \longrightarrow CO_2 + e^- \text{(to ZnO)}.$$

The EPR spectrum, as in so many of the previous studies, showed a line @ g=1.96 with a much less intense line @ g=2.002. These signals were observed after ZnO had been outgassed and annealed, however, under O_2 pressure, as before, the signals were not found even at LN_2 temperature. The signal from the outgassed, annealed ZnO was attributed to either electrons in the conduction band or interstitial zinc.

Exposure of ZnO to O_2 reduced the conductivity and the original value of conductivity could not be restored until the sample was reoutgassed above 300°C. The conductivity of ZnO was related to the O_2 species which is not readily desorbed unless the temperature exceeds 295°C and such assignment of O^- to the high temperature peak was based on the peak's behavior when the ZnO sample was exposed to CO.

To further verify this, another ZnO sample was pretreated with N_2O. When a pulse of CO was reacted with either N_2O or O_2 presorbed on ZnO below 200°C, the reaction rates were the same showing first order kinetics in CO and zero order in O_2 or N_2O.

> "Furthermore, the simultaneous competitive reaction of CO with O_2 and N_2O the reaction of CO with N_2O is strongly retarded by O_2, while the over-all carbon dioxide formation rate is the same as that observed in the separate oxidations of CO with O_2 or N_2O."

Such results suggest a common intermediate for both reactions

$$CO + \tfrac{1}{2} O_2 \longrightarrow CO_2,$$

$$CO + N_2O \longrightarrow N_2 + CO_2$$

which would reasonably be O^- [19].

In a study of temperature dependence of the resonance signal of ZnO, Sancier [20] found that the number of resonance centers increased with temperature, such centers being due either to ionized donors or conduction electrons. The donors were considered to be Zn^+ or singly ionized oxygen ion vacancies.

> "At temperatures where donor ionization becomes significant, the resonance is due mainly to conduction band electrons and to excess zinc precipitated at defects."

Of significance in this study is that the intensity of the signal @ g=1.96 was obtained such that the Q change of the spectrometer cavity was taken into account with changes in ZnO conductivity as the resonance centers increased.

In the most recent investigation of induced defects in ZnO by UV irradiation [17], a particularly noteworthy observation is made. ZnO, under UV irradiation, did not appear to change the cavity Q and did not effect the conductivity of the ZnO sample. Yet, under such irradiation, the signal intensity of the line @ g=1.96 increased markedly. If electrons under UV irradiation are promoted to the conduction band, the zinc oxide conductivity should increase and thus effect cavity Q.

> "The failure to observe a decrease in cavity Q-factor resulting from irradiation indicates that the resonance signal is not due to conduction electrons but is due to electrons at the donor level."

In summary, the EPR line for ZnO at g=1.96 has been variously attributed to Zn^{+} ions, oxygen ion vacancies, trapped electrons at oxygen vacancies, and conduction electrons in the bulk ZnO. EPR lines at g=2.01 have been attributed mainly to adsorbed species such as O_2^-, O^-, and O^{2-}. The EPR signals were strongly dependent on the method of preparation and pretreatment conditions. Appendix A gives a compilation of the zinc oxide EPR signals observed for the various experimental conditions of sample preparation, pretreatment, and substitutional ions.

EXPERIMENTAL

A. SAMPLE PREPARATION

Two methods of preparation were used for samples of indium doped ZnO. In both procedures quantities of Baker reagent grade ZnO were thoroughly mixed with In_2O_3 (indium sesquioxide) in proportions to obtain the following mole percent indium in ZnO:

1.0 mole % In in ZnO
0.5 mole % In in ZnO
0.1 mole % In in ZnO
0.05 mole % In in ZnO
0.01 mole % In in ZnO
0.005 mole % In in ZnO

Indium sesquioxide was prepared from the metal by firing in a crucible until ignited. This partially oxidized material was then placed in a furnace for 72 hours at 1100°C to complete the oxidation process.

In the first method, a small quantity of the 1 mole percent In_2O_3-ZnO mixture was pressed at 6000 lbs. in a 0.25 inch diameter iron dye into a pellet and sintered in a furnace at 1300°C for various lengths of time from 2 to 28 hours. These pellets were then broken up and ground to a powder in an agate mortar for EPR measurement.

In the second method, samples of all the listed percentages of indium in ZnO were prepared by vapor transport. This method of crystal growth has been described in the literature [21, 22, 23]. The furnace used was a Lindberg HEVIDUTY type 54258 tubular furnace configured with a four foot mullite

tube with an inside diameter of 1.5 inches. The furnace temperature was controlled with a Lindberg type 59545 controller which regulated the temperature within ±2°C. The temperature on the inside of the mullite tube was 20°C below the controller setting when set in the range from 900°C to 1300°C. There was no temperature gradient over the distance between the starting material cylinder and the doped crystal deposit site.

About 100 grams of the oxide mixture was made into a cylinder and sintered for 4 hours @ 900°C. This cylinder was then placed in the furnace. The furnace temperature was regulated at 1100°C and the mullite tube was stoppered at one end with a Teflon stopper wrapped in asbestos. Two quartz tubes through the Teflon stopper carried the reacting gasses. The cylinder of mixed oxides was placed about 18 inches from the end of the mullite tube, downstream of the point where H_2 entered. In this way the oxide cylinder was well bathed with H_2, which reduced the oxides to metal vapor. The vapor was then carried down the furnace tube to the point where O_2 could reoxidize the vapors. A second cylinder of pure ZnO was provided as a growth site for the crystals of ZnO-In. This was placed about 4 inches away from the first (figure 1). A one-to-one ratio of H_2-O_2 was used and N_2 was provided in order to vary total flow rate (figure 2). After about 5 minutes of growth, the large ZnO cylinder with the ZnO-In crystals was withdrawn from the furnace and allowed to cool in air to room temperature. Some crystal growth also occurred

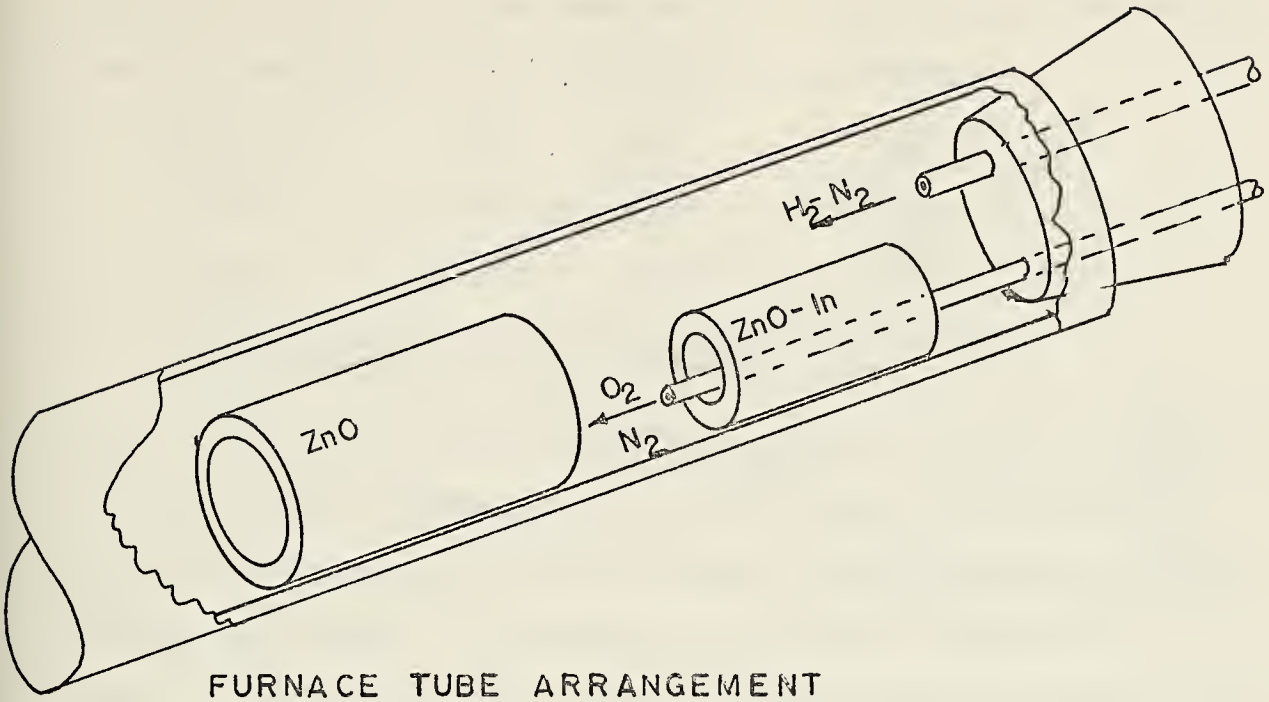

FURNACE TUBE ARRANGEMENT

FIGURE 1

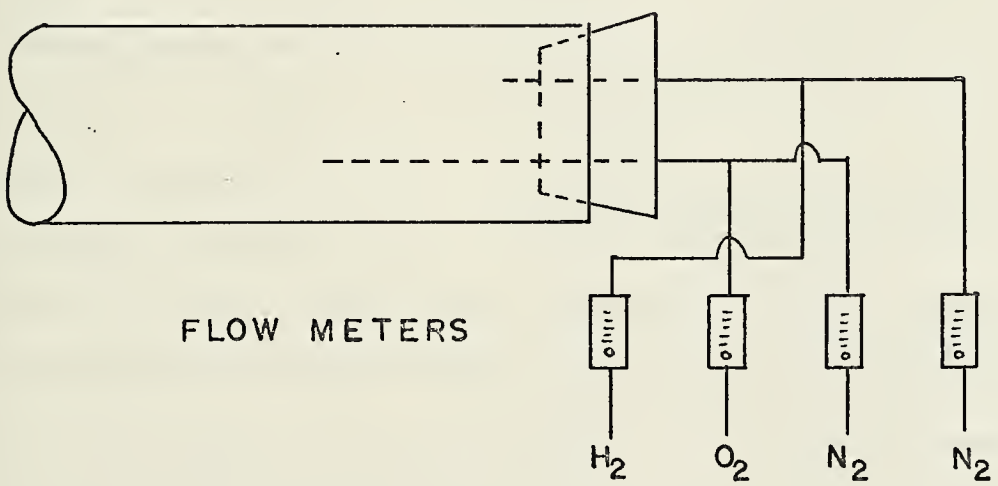

GAS FLOW CONTROL

FIGURE 2

on the end of the O_2 tube which was also withdrawn from the furnace to cool at room temperature. Good crystal growth rate was obtained with the following gas flow rates:

Temp °C	H_2*	N_2*	O_2*	N_2*
1100	0.45	2.0	0.5	--
1150	1.00	1.00	1.0	0.5

* Flow rates are in cubic feet per hour (CFH).
1 CFH = 7.865 ml/sec.

Both these conditions produced crystals of about 1 to 2 mm in length with a diameter of 0.1 to 0.2 mm. The crystals were not uniform and the growth habit was dependent on the doping percentage. In general the crystal shape was as shown in figure 3. The higher the percentage of indium, the shorter and less uniform were the crystals, both in color and form. At low percentages of indium (<0.01 mole percent) the crystals were light blue with increasing hue as the doping level increased. At the higher percentages the crystals were motley with dark blue, light blue and yellow-green areas throughout. In contrast, samples prepared by the first method (1.0 to 0.05 mole % In) in pellet form varied only in hue from light to dark yellowish-green depending on the length of time sintered.

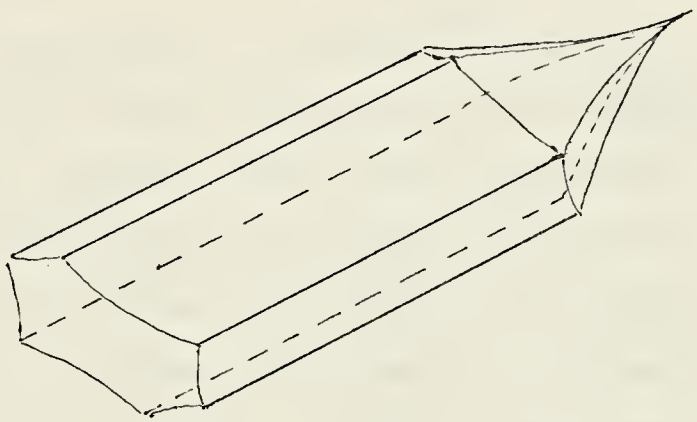

Indium Doped ZnO Crystal
Figure 3.

In addition to vapor grown doped samples, undoped vapor grown ZnO was prepared using various ratios of H_2-O_2 in order to produce ZnO in an oxygen rich and oxygen poor condition.

The samples prepared as described above were from reagent grade ZnO containing small but significant amounts of impurities, both donors and acceptors. To obtain higher purity ZnO, some pellets were made from 99.99 percent Zn. The metal was ignited in air to complete oxidation and subsequently mixed with In_2O_3. Pellets of this material were made in the same way and subsequent treatment was the same as for the reagent grade materials.

B. INSTRUMENTAL ANALYSIS

Light absorption measurements in the infra-red were carried out using a Perkin-Elmer grating infra-red spectrometer, Model 337, with a tungsten light source and photomultiplier detector, and in the UV and visible portions of the spectrum a Beckman DK-1A dual beam grating spectrophotometer with a hydrogen or tungsten light source as appropriate and PbS or photomultiplier detector. The wave length range scanned on the Beckman instrument was from 0.18μ to 4.0μ and on the Perkin-Elmer from 2.5μ to 25μ.

Determination of indium in vapor grown ZnO was made by using a Perkin-Elmer, Model 303, dual beam Atomic Absorption spectrometer. With an indium hollow cathode lamp (Perkin-Elmer 303-6034 M-1457) as a source and using an air-acetylene flame with a three-slot burner, the indium line at 3039Å

proved to be the most sensitive. Spectrometer slit settings and gas flow rates were according to the Perkin-Elmer recommended settings (Analytical Methods for Atomic Absorption Spectroscopy, 1971).

A working curve was developed for indium in a high Zn, high chloride environment which showed good linearity up to 25 ppm with only slight deviation from linearity up to 40 ppm (figure 4). All standards contained 0.0803 grams Zn per milliliter in 6M HCl corresponding to quantities expected for the unknown samples such that the observed concentration of indium would fall in the region from 5 ppm to 25 ppm. The unknown samples were dissolved in 6M HCl, some of which required mild heating.

The EPR measurements were carried out using a Varian, Model V4502, EPR spectrometer operating in the 9.4-9.6 GHz (X-band) range. The microwave cavity was operated in the TE_{102} mode with a modulation frequency of 100 kHz. The magnetic field was from a 9 inch magnet regulated to within ±0.1 gauss. The cavity was configured with a Varian temperature controlled dewar assembly for temperatures ranging from 93°K to 540°K. Temperature measurements were made with a calibrated copper/constantan thermocouple.

Spin density measurement standards used were (1) freshly recrystallized $CuSO_4 \cdot 5H_2O$ for room temperature and below, and (2) Varian 0.1% pitch in KCl for temperatures above 300°K. Comparison of spin density of $CuSO_4 \cdot 5H_2O$ with 1 cm of $3X10^{-4}$% pitch in KCl (Varian) showed agreement with the theoretical

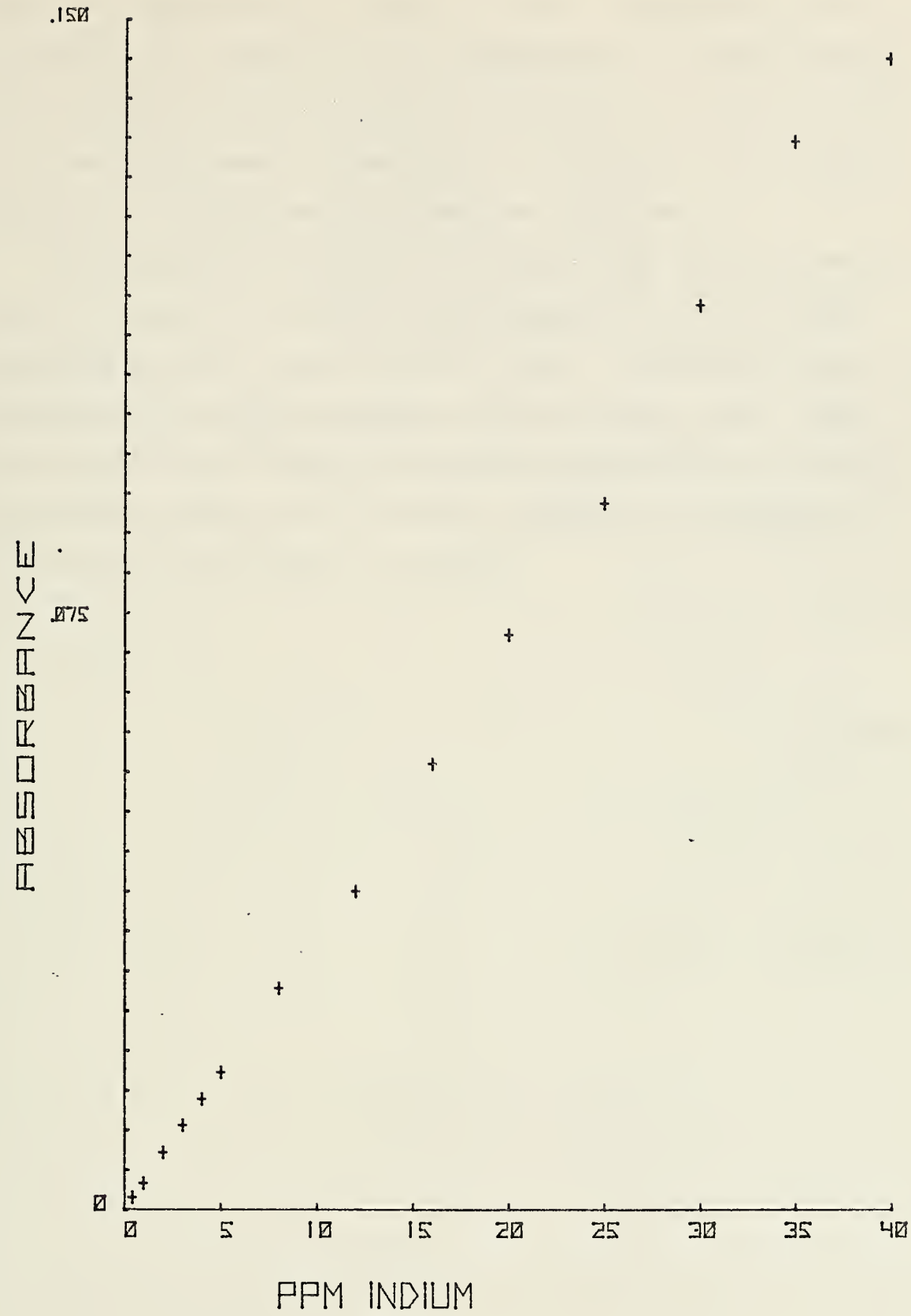

FIGURE 4

number of spins within a factor of two. The weight of indium doped ZnO used was 2 to 6 milligrams. All spin density values reported from intensity calculations are within ±30% and from first moment calculations within ±10%. The g-value accuracy is ±0.0002 unless otherwise indicated.

The apparatus used when the samples were under vacuum is shown in figure 5. Pressure measurements at the ion gauge ranged from $1X10^{-6}$ Torr to $3X10^{-7}$ Torr. Considering the distance of the gauge and pump from the sample tube, there may be one or two orders of magnitude difference in pressure between the gauge and the sample, therefore, a pressure of 10^{-5} Torr at the sample is assumed.

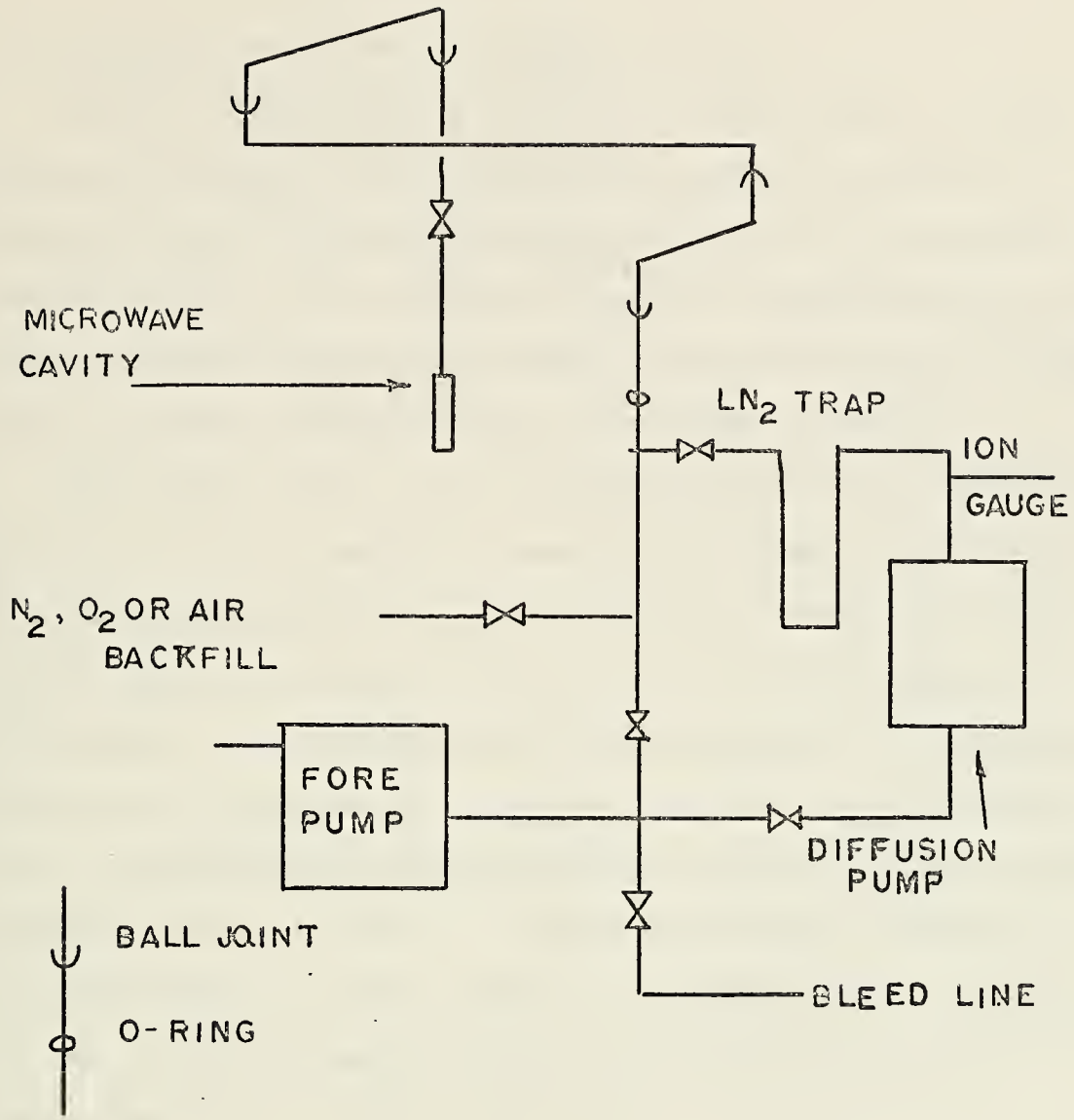
MICROWAVE
CAVITY
LN_2 TRAP
ION
GAUGE
N_2, O_2 OR AIR
BACKFILL
FORE
PUMP
DIFFUSION
PUMP
BALL JOINT
O-RING
BLEED LINE

FIGURE 5

RESULTS AND DISCUSSION

A. INDIUM ANALYSIS OF VAPOR GROWN ZnO-In

Indium doped crystals of ZnO were vapor grown, as previously described, from mixtures containing various mole percent indium. As would be expected [24, 25], increased percent indium in the starting material yielded vapor grown products in which the color varies from blue to yellow/green. Indium analysis results are given in Table I.

The indium found in the samples prepared from zero percent In is due to residual amounts of indium in the furnace. Although after each run in which doped crystals were made the furnace was scrubbed with H_2 for periods as long as 20-30 minutes, small amounts of indium remained. In addition, as the ZnO collector cylinder was used the blue coloration due to indium doping became quite noticeable, thus providing another source of indium. Further verification for the presence of In in these samples came from the EPR signal at g=1.96 which for reagent grade ZnO is very weak but for these samples was readily apparent.

The data in Table I show that the concentration of indium in vapor grown ZnO is, in general, of the same magnitude as the concentration of indium in the starting material. This indicates that the vapor growth technique may be used to dope ZnO with doping levels being controlled by the percentage of dopant used in the starting material mixture.

CONDITIONS OF CRYSTAL GROWTH

Sample	Starting Mole % In	Analyzed Mole % In	Temp°C	Gas Flow Rates N_2	O_2	N_2	H_2	Crystal Color
10F	0.0	0.0031	1150	-	0.5	2	0.45	White
8A	0.0	0.0040	1150	-	0.5	2	0.45	Very Light Blue
10E	0.0	0.0041	1150	-	0.5	2	0.45	White
8F	0.01	0.0052	1150	-	0.5	2	0.45	Very Light Blue
8G	0.01	0.0062	1150	-	0.5	2	0.45	White/Light Blue
8B	0.0	0.0098	1150	-	0.5	2	0.45	Very Light Blue
5F	0.005	0.0117	1100	0.5	1	1	1	Light Blue
6D	0.01	0.019	1100	0.5	1	1	1	Blue
9C	0.1	0.0602	1150	-	0.5	2	0.45	Light Blue
9D	0.01	0.0828	1150	-	0.5	2	0.45	Blue
6C	0.0	0.085	1100	0.5	1	1	1	Blue/Green
6E	0.1	0.137	1100	0.5	1	1	1	Dark Blue/Blue Green
9G	0.5	0.369	1150	-	0.5	2	0.45	Dark Blue/Yellow
10A	0.5	0.526	1150	-	0.5	2	0.45	Yellow-Green

Table I

Indium Doped Zinc Oxide Crystal
Growth Conditions and Indium Analysis

B. LIGHT ABSORPTION OF ZnO-In

According to Bogner et al [24], indium doped single crystal ZnO has a strong absorption in the far infra-red which with increased conductivity, moves into the near infra-red and visible region of the spectrum. The shift in absorption with increased conductivity produces a blue color in the crystal. In substantial agreement with this observation, Kasper [25], using polycrystalline indium doped ZnO in reflectance spectroscopy, observed that with increased conductivity a definite shift of the absorption edge toward the visible occurred (figure 6). At low concentrations the transmittance in the visible is virtually 100 percent but as the concentration of indium increases and the absorption edge moves closer to the UV, the compound appears either green or yellow. Kasper [25] also found the line at g=1.95 in the EPR spectrum, which he attributed to free electrons.

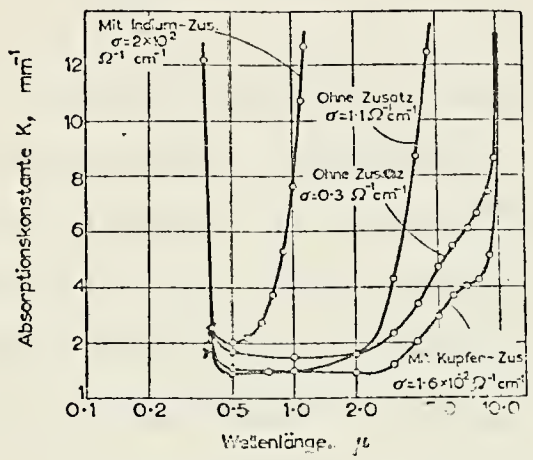

Reflectance Spectra of ZnO-In

Figure 6.

For polycrystalline semiconducting materials, light absorption due to free electrons will occur in the infra-red region, and in the IR-visible-UV spectra the absorbance is proportional to the number of free electrons which, in indium doped ZnO, increase with higher temperatures, and decrease as the O_2 partial pressure is increased [3, 25].

A quantitative comparison of transmittance spectrum of indium doped ZnO and the EPR intensity of the line @ g=1.96 could, in light of the preceding observations, provide a simple measure of the conductivity of polycrystalline ZnO-In from an EPR measurement.

In order to test this concept, two samples of vapor grown indium doped ZnO (0.05 mole percent and 1.0 mole percent) were prepared and ground to a fine powder. This powder was thoroughly mixed with spectral grade KBr and pressed into a pellet. The pellets were prepared quantitatively in a 10:1 KBr: ZnO-In ratio. These spectra are shown in figures 7 and 8.

In view of the high (1.0%) concentration used in one of the samples having a yellow/blue appearance, absorption should be expected in the UV and visible. The absence of a well defined absorption must be attributed to the experimental technique where the size of the ground particles and the pellet formation were not well controlled. Presumably when the pellet was pressed at 27,000 lbs. the KBr did not properly fuse around the ZnO-In crystals leaving cracks in the pellet. These cracks then scattered the incident light so severely that any quantitative measure could not be achieved. With smaller crystals (i.e., on the order of a micron) fusing of KBr around the particles may be achieved and hence transmittance spectroscopy may be possible. But, the results of commercially prepared powdered ZnO does not appear to be encouraging (figure 9).

This avenue was not pursued further.

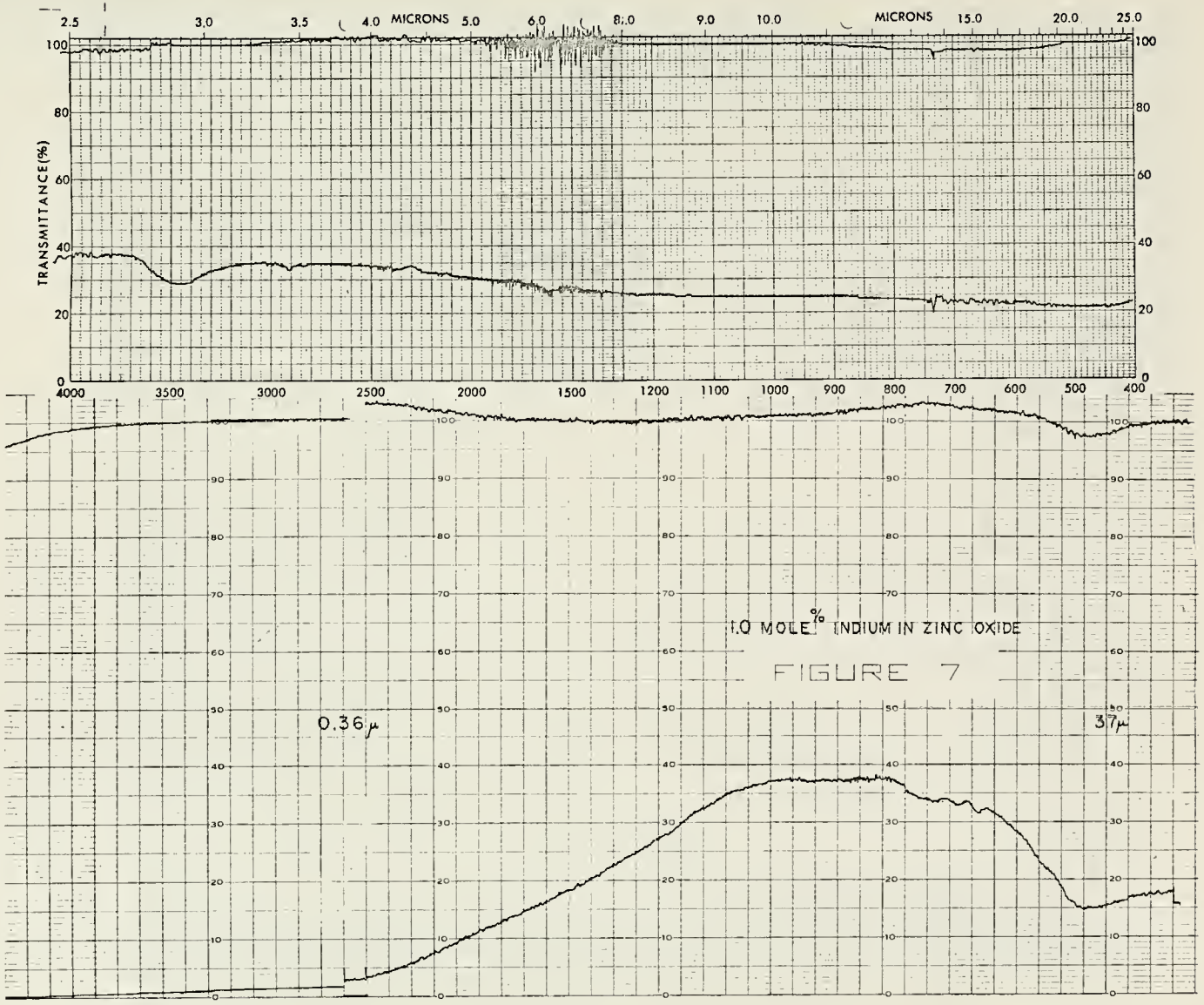

1.0 MOLE % INDIUM IN ZINC OXIDE

FIGURE 7

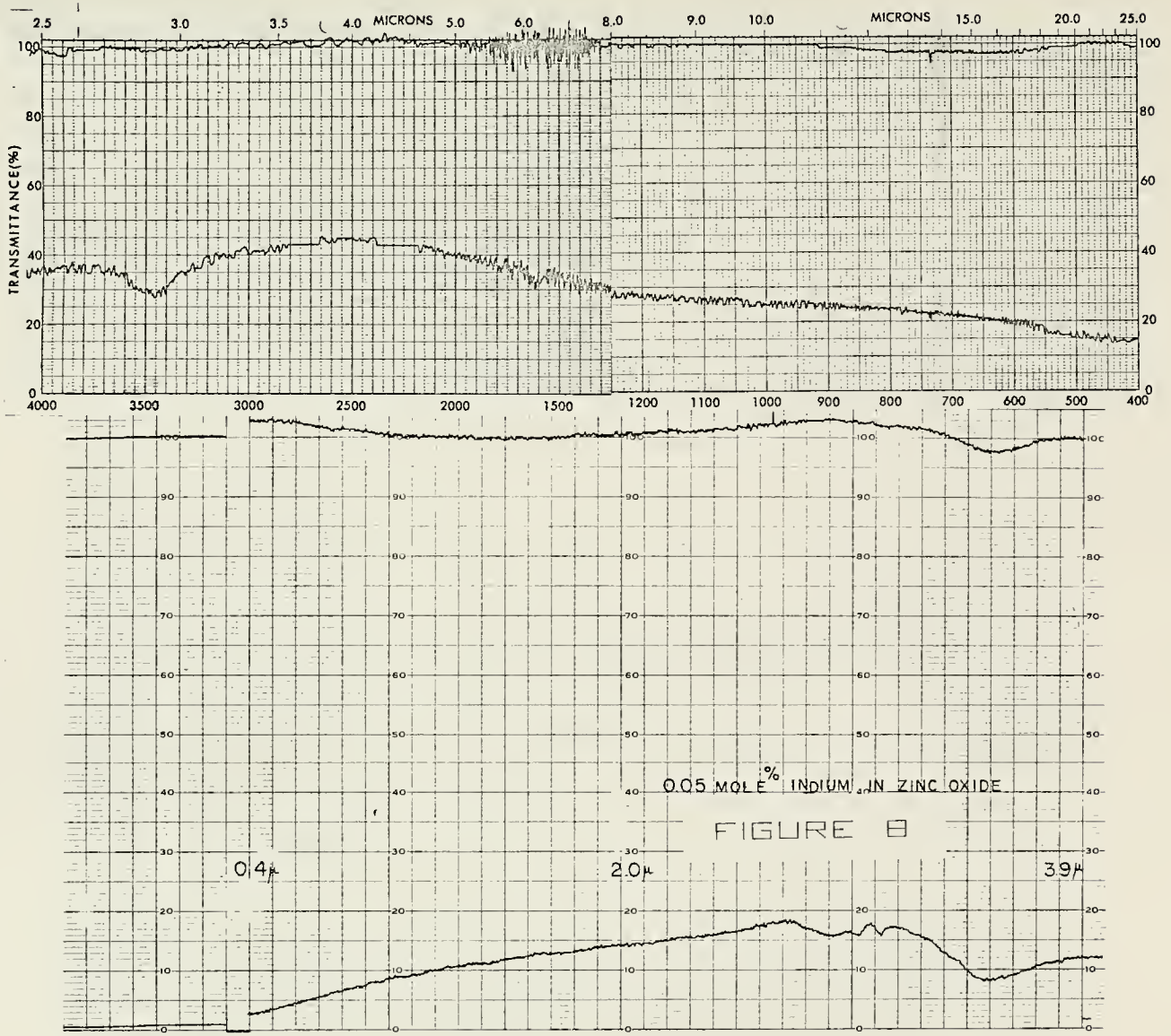

0.05 MOLE % INDIUM IN ZINC OXIDE

FIGURE 8

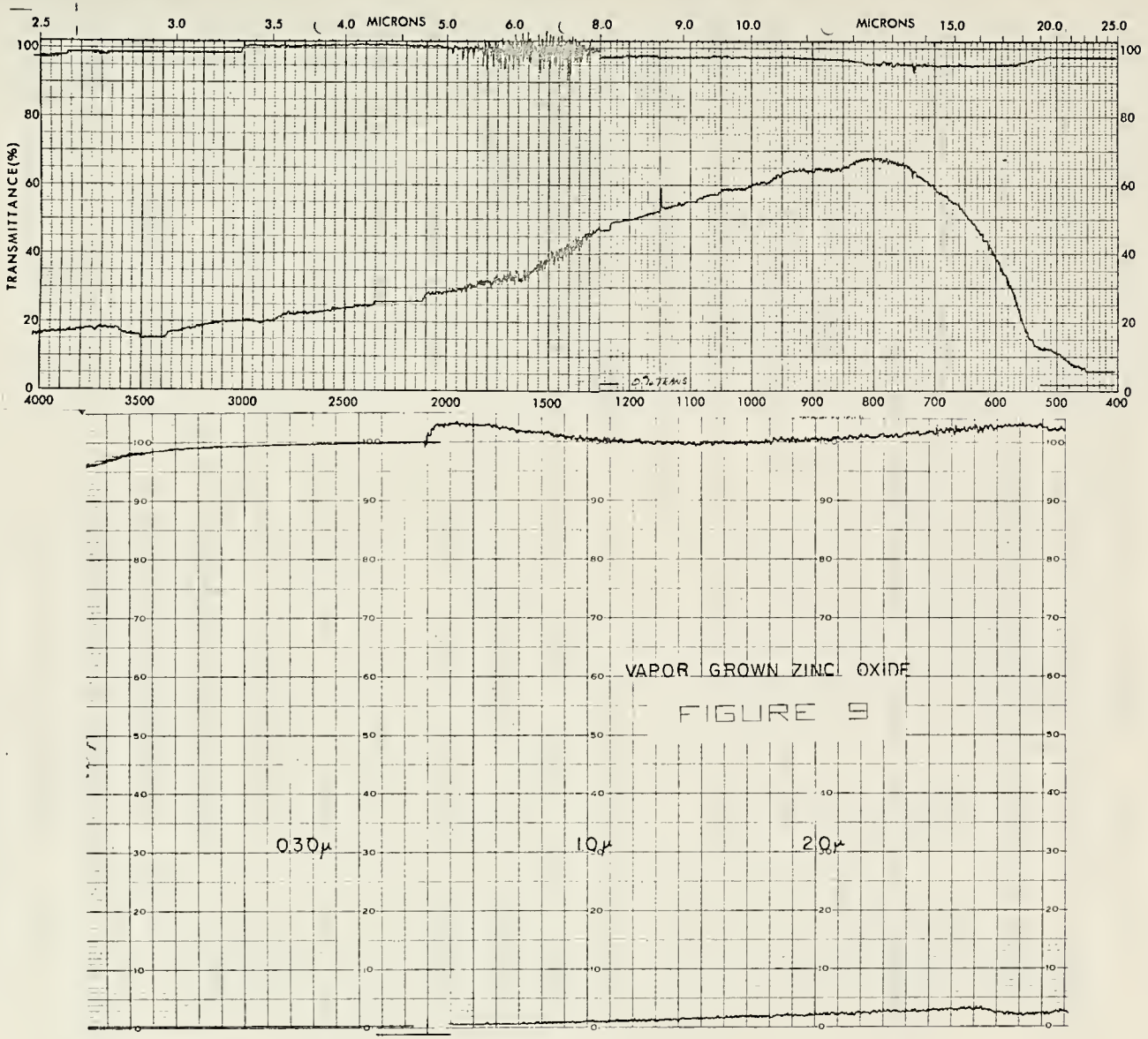

VAPOR GROWN ZINC OXIDE

FIGURE 9

C. EPR OF MECHANICALLY DAMAGED ZnO

In order to evaluate the effect of sintering of the $ZnO-In_2O_3$ mixtures which had been formed into pellets, the EPR spectrum before sintering was obtained. When an unsintered pellet was broken up and lightly ground to a powder, three lines @ g=2.01 in the EPR spectrum (figure 10) were observed. This signal was, in addition to a weak signal @ g=1.96, found in unstressed reagent grade and high purity ZnO. EPR signals in the vicinity of g=2.01 have been reported for ZnO subjected to various O_2 and other gas pretreatment conditions, but particularly under conditions arising from mechanical stress [4, 15, 17, 26]. These same three lines were induced by grinding of reagent grade and high purity ZnO in an agate mortar until the white ZnO becomes yellow under the stressing conditions. The intensity of the EPR signal was independent of the pressure applied when pellets were prepared at pressures above 3000 lbs. but was markedly less below this pressure. As long as the yellow color was present in mechanically stressed ZnO, the signal was present. However, when a pellet was sintered @ 1100°C and then lightly ground to a powder, the signal was not detectable. Vapor grown ZnO ground to a powder also yielded the yellow color and gave a similar EPR spectrum. When indium doped vapor grown ZnO was treated in the same way it was possible to obtain the three lines as well, but considerably more effort in grinding was required and the signal intensity was much less (figure 11).

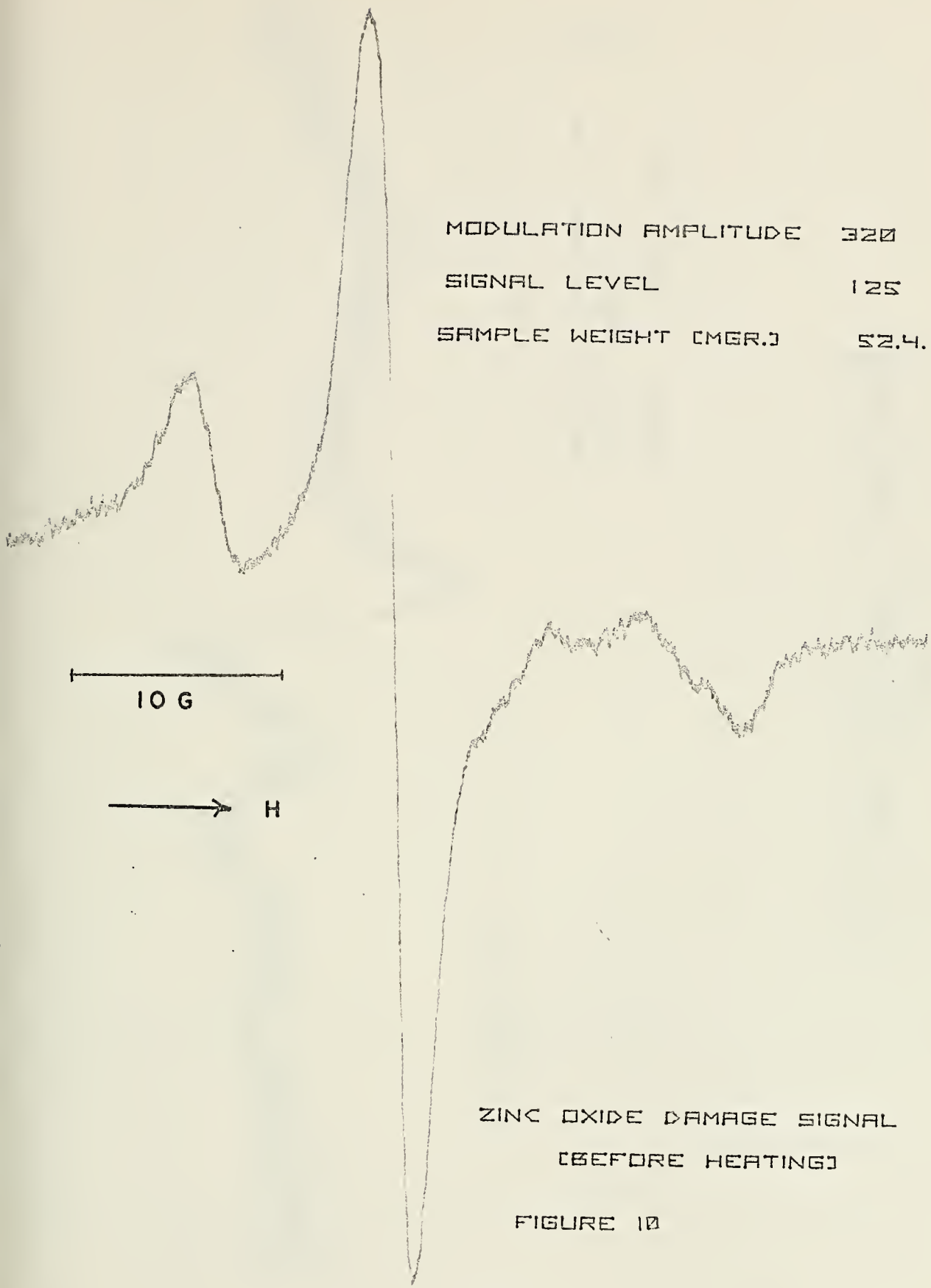

ZINC OXIDE DAMAGE SIGNAL
(BEFORE HEATING)

FIGURE 10

MODULATION AMPLITUDE	320
SIGNAL LEVEL	500
SAMPLE WEIGHT (MGR.)	15.

INDIUM DOPED ZINC OXIDE DAMAGE SIGNAL

FIGURE 11

Sancier [15] and Golubev et al [26] report that the signal in undoped mechanically stressed ZnO disappeared upon evacuation and heating above 375°K. In these experiments it was not found necessary to evacuate a sample if sintered at 1100°C in order for the signal to be undetectable but the three lines in the EPR spectrum did not disappear when the sample was evacuated to 10^{-4} Torr for 3.5 hours.

The g-values of the three lines were 2.0052, 2.0136, and 2.0184±0.0002 in substantial agreement with previously reported values [4, 15, 17] with the exception of those observed by Golubev [26], who reports the three lines about two gauss downfield. The behavior under vacuum and heating is, however, substantially the same in each case. The length of time of heating of the sample was not reported in the referenced studies but the disappearance of the three lines apparently occurred rapidly. In this study the three lines are not detectable after heating for as little as 15 minutes, but when the sample was heated for a period of only 30 seconds with a flame estimated to raise the temperature of the sample to about 400°-450°K, the behavior of the EPR signal was different. Under these conditions the three lines were no longer in evidence but were replaced by an isotropic singlet with a g-value not corresponding to any of the previously observed three lines. This singlet had a g=2.0109±0.0003 (figure 12).

Consideration of the three lines as being due to a single species led to an attempt to align vapor grown ZnO needles and press them into a pellet. The resulting pellets did not

MODULATION AMPLITUDE	320
SIGNAL LEVEL	100
SAMPLE WEIGHT (MGR.)	52.4

ZINC OXIDE DAMAGE SIGNAL (AFTER HEATING)

FIGURE 12

provide enough samples for either the three line damage signal or the signal at g=1.96 to be detectable. A similar attempt with some large crystals in KBr was equally unsuccessful.

In view of the fact that a singlet remained after quick heating it does not seem likely that the paramagnetic centers induced by mechanical stressing are due to a single species, but rather, the three lines are due to the interaction of various surface adsorbed species and surface defects in ZnO. At room temperature, desorption of these adsorbed gasses does not readily occur. Whereas at high temperatures prolonged heating provides sufficient energy to restore the defects and heating at 375°K allows some of the surface adsorbed gasses to be desorbed, the quick heating probably causes desorption of certain adsorbed species leaving a single less readily desorbed species behind to interact with the surface defects. The shift in g-value for this singlet further suggests that the three lines are not a triplet associated with a single species.

In indium doped ZnO the availability of electrons for capture by surface adsorbed species would be greater than for the undoped material. This would shift the equilibrium of adsorbed species and alter the relative intensities of the three lines.

D. EPR OF ZnO-In

The EPR spectrum of indium doped ZnO is a single, slightly anisotropic line @ g=1.957 (figure 13). The anisotropy

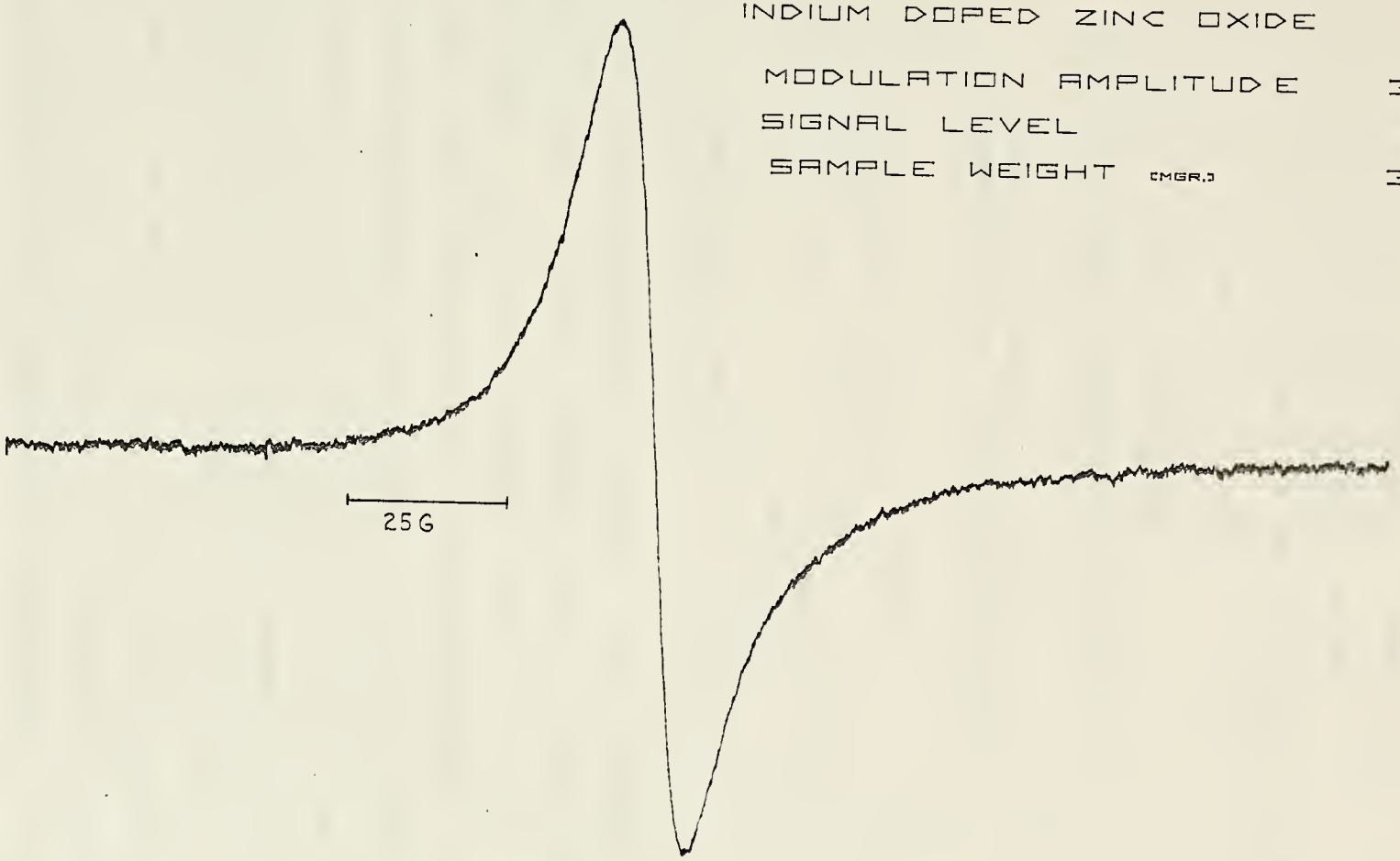
INDIUM DOPED ZINC OXIDE
MODULATION AMPLITUDE 320
SIGNAL LEVEL 80
SAMPLE WEIGHT (MGR.) 3.7
25G

FIGURE 13

was independent of the dopant concentration, temperature and pressure. The most significant changes which occurred, depending on the dopant concentration, temperature, and the pressure, were the line width and g-value.

In order to clarify what is meant by certain terms, the following definitions will be used:

M ≡ first moment (APPENDIX B)

M* ≡ first moment corrected for change in spectrometer cavity Q

I ≡ intensity, calculated assuming Lorentzian line shape; $(\text{line width})^2 \times$ (line height)

I* ≡ intensity corrected for change in spectrometer cavity Q

h ≡ line height; peak to peak perpendicular distance of the first derivative

w ≡ line width; first derivative peak to peak width in Gauss

Corrections for change in cavity Q were obtained by comparison with a standard, assuming that, as in the case of $CuSO_4 \cdot 5H_2O$, $M_{CuSO_4} T$ is a constant [20].

EPR spectra were obtained of vapor grown ZnO-In samples for which the indium concentration had been determined, and the results are tabulated in Table II. Since these samples were prepared at 1100°C and quenched, supersaturation of In in ZnO should result [3]. When a 0.01 mole precent In in ZnO sample was prepared in this way, the EPR spectrum was a single line with a line width of 14.96 gauss, g=1.9580 and spin density of $5X10^{19}$ spins/mole (sample B10). A second sample was prepared in the same way except that upon completion of vapor growth the crystals were left in the furnace

Sample	Analyzed Indium Concentration (mole %)	Spin Density Calculated From M*ZnO-In X10-19	Spin Density Calculated From I*ZnO-In X10-19	Line Width w (Gauss)	g-value ±0.0002
10F	0.0031±0.0005	2	0.9	5.70	1.9565
8A	0.0040±0.0005	-	4	7.20	1.9563
10E	0.0041±0.0005	1	0.8	6.50	1.9564
8F	0.0052±0.0005	3	3	7.66	1.9566
8B	0.0098±0.0005	2	1	8.70	1.9566
5F	0.011 ±0.001	4	3	8.70	1.9575
6D	0.019 ±0.001	4	2	8.66	1.9572
9C	0.060 ±0.001	7	9	11.02	1.9581
9D	0.082 ±0.001	8	6	10.80	1.9582
6C	0.085 ±0.001	4	3	9.19	1.9572
6E	0.137 ±0.005	5	3	12.40	1.9578
9G	0.369 ±0.005	6	8	18.26	1.9591
10A	0.526 ±0.005	6	6	15.45	1.9581

Table II

Indium doped zinc oxide spin densities, line widths and g-values at room temperature and atmospheric pressure.

and the furnace turned off to cool to room temperature over a period of about 24 hours. These annealed crystals gave an EPR spectrum of a single line, but the line width was narrower, (w=7.70 gauss) and the g-value and spin density lower (g=1.9570, spin density=$8X10^{18}$ spins/mole for sample B12). The appearance of the crystals in sample B10 was blue with some yellow, whereas sample B12 was uniformly light blue. This is to be expected since the diffusion of indium out of the crystal can occur under annealing conditions but when quenched the crystal is supersaturated with indium [3]. This may further be substantiated with reference to the color condition which was similar to that observed by Kasper [25]. Conductivity measurement on small single crystals of B10 yielded $\rho=2.4\pm0.5\Omega cm$. Similar measurements on B12 were not reproducible but showed generally higher resistivity.

The microwave skin depth is not a limiting factor in these and other spin density measurements. Since for crystals with resistivity of $1\Omega cm$, the microwave skin depth at 10GHz is 0.5 mm, with crystal diameters generally less than 0.1 mm and resistivities on the order of $1\Omega cm$, it is expected that the penetration of the microwaves is not inhibited. In addition, only slight anisotropy was observed for the EPR signal at g=1.957 [27, 28].

When polycrystalline ZnO was outgassed at high temperature and maintained under vacuum, the intensity of the EPR line @ g=1.96 increased; this was attributed to electrons being returned to the ZnO by desorption of O_2^- or O^- species

Temp °K	Arbitrary Units $M^*_{ZnO-In^T}$	$I^*_{ZnO-In^T}$	Line Width w (gauss)
93	1.2	1.2	5.50
123	4.0	2.0	6.17
145	5.1	2.5	7.00
171	5.5	3.8	8.67
198	5.7	3.5	9.17
224	6.3	4.3	10.00
251	7.3	3.8	9.50
273	6.6	6.2	11.73
294	7.1	4.0	11.67

Table III

Sample 6E at p=760 mm Hg

Temp °K	g-value	Arbitrary Units $I^*_{ZnO-In^T}$	Line Width w (gauss)
118	1.9573	1.0	3.30
151	1.9573	1.2	4.07
178	1.9572	1.7	5.07
206	1.9572	2.9	6.90
228	1.9572	4.1	8.20
239	1.9572	3.6	8.20
259	1.9573	4.1	8.14
273	1.9573	6.6	9.24
296	1.9574	5.9	8.93

Table IV

Sample 6D at p=760 mm Hg

[5, 8, 10, 19]. When indium doped ZnO was similarly outgassed at 837°K and 10^{-4} Torr for at least two hours no measurable intensity change occurred when the EPR spectrum was obtained at room temperature.

In the single crystal indium doped ZnO conductivity work done by Bogner and Mollwo [24], the conductivity of the crystals was proportional to the indium concentration to about 0.2 mole percent indium. Above this concentration the conductivity was a constant (figure 14). If the spin density is proportional to the number of electrons in the conduction band it is then proportional to the conductivity. However, a plot of spin density versus dopant concentration (figure 15) does not show linear correlation with the curve in figure 14. Although there is scatter in the data, a one-third dependance is evident.

In his work on powdered ZnO, Sancier [20] found that when under vacuum $M^*_{ZnO}T$ was not a constant but rather increased with temperature. In that study, Zno was pretreated by outgassing at high temperature under vacuum, sealed off, and EPR measurements made from @ 90°K-500°K. With this temperature dependence in mind, In doped ZnO samples (6D and 6E) were investigated at varying temperatures. The results are given in Tables III and IV. The samples were at atmospheric pressure and $CuSO_4 \cdot 5H_2O$ was used as a standard to correct for cavity Q changes due to changes in the sample conductivity [20]. Under these conditions the behavior of the $M^*_{ZnO-In}T$ (figure 16) and $I^*_{ZnO-In}T$ (figure 17) for

FIGURE 14

LOG10 MOLE PERCENT INDIUM
0
-1
-2
-3
LOG10 SPIN DENSITY (SPINS/MOLE)
20.
19.5
19.

FIGURE 15

M_{ZN-DT}^{*} (AT ATMOSPHERIC PRESSURE)
0
.1
.2
.3
.4
.5
.6
.7
.8
.9
1.0
0
100
200
300
TEMPERATURE °K

FIGURE 15

ZN-D T [AT ATMOSPHERIC PRESSURE]
TEMPERATURE V
0
1
2
3
4
5
6
7
8
9
10
0
100
200
300

FIGURE 17

sample 6E was qualitatively the same as Sancier [20] had observed for his undoped samples. The scatter in $I^*_{ZnO-In}{}^T$, however, puts this method of obtaining the intensity [5] in some doubt. The plot in figure 18 for $I^*_{ZnO-In}{}^T$ of sample 6D does not show the same curvature as sample 6E but the increase with temperature is still evident.

The data for sample 6D under vacuum from low and high temperature measurements are tabulated in Tables V and VI, respectively. The range in M*T with temperature for the low temperature range is not as great as when the sample was at atmospheric pressure (cf figure 16 and figure 19), and similarly, the line narrowing was not as marked (figure 20). The last two entries in Table V are of interest because a marked decrease in line width occurred when air was admitted to the sample tube. The line height on the other hand increased such that the spin density of the sample remained the same within experimental error.

In the high temperature region the results are not as clear. As the temperature was increased vibrations from the pumping system were more noticeable and at the higher temperatures, interfered markedly. In general, the noise in the system when the temperature was above 370°K was such as to cast some doubt on that data. The trend toward broader lines, however, remained as the temperature was increased.

Since a plot of M*T for ZnO [15] and a similar plot for indium doped ZnO do not yield a straight line with zero slope the electrons giving rise to the EPR spectra are not localized

Temp °K	g-value	Arbitrary Units $M^*_{ZnO-In^T}$	Line Width w (Gauss)
96	1.9575	1.3	7.48
104	---	1.2	7.60
168	---	1.5	8.00
197	1.9574	1.5	8.10
229	---	1.8	9.23
260	1.9581	1.9	9.56
298	1.9577	1.7	10.77
298 (Note 1)	1.9575	-	9.45
96 (Note 2)	1.9575	1.0	3.51

Note 1: at atmospheric pressure.
Note 2: this point obtained with the sample at atmospheric pressure following the previous vacuum treatment.

Table V

Sample 6D - Under Vacuum @ 10^{-5} Torr

Temp °K	g-value	Arbitrary Units $I^*_{ZnO-In^T}$	Line Width w (Gauss)
298 (Note 1)	1.9583	1.5	9.70
298	1.9577	1.2	11.76
313	1.9578	1.0	10.81
349	1.9579	2.1	12.51
371	1.9580	1.9	12.00
400	1.9581±0.0005	2.2	13.43
429	1.9582±0.0005	-	12.34
471	1.9582±0.0005	4.3	16.59
523	1.9585±0.0005	3.2	15.48
298 (Note 2)	1.9570±0.0005	1.1	10.58
298 (Note 3)	1.9569±0.0005	-	9.05

Note 1: sample at atmospheric pressure.
Note 2: sample was heated to 837°K in vacuum and cooled in air to room temperature under vacuum.
Note 3: sample is the same as in Note 2 but at 760 mm Hg air.

Table VI

Sample 6D - Under Vacuum @ 10^{-5} Torr

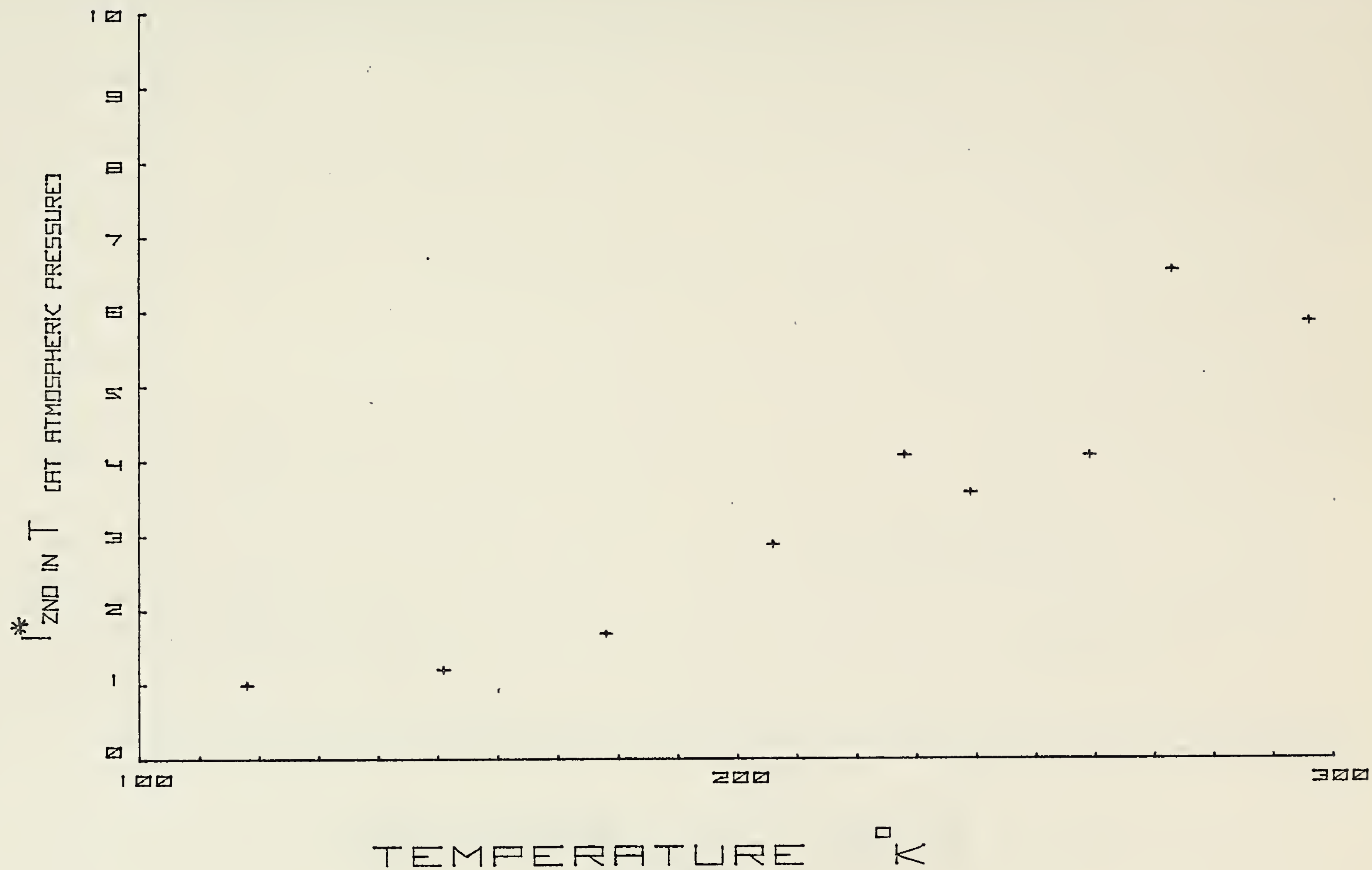

FIGURE 18

M* ZND-IN T (UNDER VACUUM)
2.0
1.9
1.8
1.7
1.6
1.5
1.4
1.3
1.2
1.1
1.0
50
200
300
TEMPERATURE °K

FIGURE 19

LINE WIDTH [GAUSS]
11
10
9
8
7
6
5
4
3
2
1
0
50
200
300
TEMPERATURE °K
+ UNDER VACUUM (10⁻⁵ TORR)
□ AT ATMOSPHERIC PRESSURE

FIGURE 20

and non-interacting. If the electrons are conduction electrons, M* should be a constant with temperature. Therefore, it cannot reasonably be assumed from observation of the M* vs. T curve for indium doped ZnO (figure 21) that the electrons are in a conduction band. Furthermore, when ZnO was irradiated with ultraviolet light, the failure to observe changes in the EPR spectrometer cavity Q led Mookherji [17] to conclude that the electrons responsible for the UV induced resonance existed in a donor band. In the same study he also observed an increase of line width of the UV induced signal with temperature similar to the dependence seen in figure 22 for indium doped ZnO at atmospheric pressure. And since the donor band in donor doped ZnO lies just below the conduction band [1] the availability of electrons to adsorbed species at the surface may still be accounted for.

Müller and Schneider [1] state that when there is sufficient overlap of the essentially s-character donor band wave functions, the hyperfine structure in the EPR spectrum of indium doped ZnO will not be observed. The onset for sufficient overlap to occur was estimated to be about an order of magnitude below the concentration of indium in the vapor grown ZnO in this study. As the concentration of donors increases, the donor band broadens until the indium donor band wave functions overlap the ZnO conduction band wave functions so as to become indistinguishable. The estimate of Müller et al [1] is that for ZnO-In this will occur @ $9X10^{19}$ donor atoms per mole. A plot of spins per mole, assuming one electron per atom yields the dotted line shown in figure 15.

TEMPERATURE
FIGURE 21
V
M
ZND-IN
(AT ATMOSPHERIC PRESSURE)
0
50
100
200

LOG10 MOLE PERCENT INDIUM
LINE WIDTH (GAUSS)
0
-.5
-1.0
-1.5
-2.0
0
-.5
-1.0
-1.5
-2.0

FIGURE 22

As the concentration of indium in ZnO increases, the donors get closer to each other and spin pairing may occur. Since the EPR signal intensity is proportional to the number of unpaired electrons the spin density would be expected to decrease relative to the donor concentration. Thus the observed behavior of spin density in figure 15 would not be, as suggested by the slope, a one-third dependence, but rather represent a more complex relationship to concentration.

Since, according to the Elliot relaxation mechanism [28] it is expected that conduction band electron EPR line width will be narrower than for donor band electrons, the trend toward broader lines with increasing dopant concentration (figure 22) does not support assignment to the conduction band. The behavior of the g-value in this respect is not explained (figure 23).

As the dopant concentration in indium doped zinc oxide increases so does the line width of the EPR signal (figure 22). This same trend is evident in the increase of g-value with dopant concentration (figure 23). These effects may be due either to changes in the equilibrium of adsorbed species or crystalline lattice changes due to the larger indium ions. Since the materials studied here are of significantly less surface area than those studied by Sancier it would not be expected that such large changes in the EPR spectrum could be entirely due to the surface adsorbed species. And yet, the observation that the increase in spin density with temperature for samples under vacuum is much less than for those

LOG10 MOLE PERCENT INDIUM
G VALUE
0
-1
-2
-3
.9550
.9600
.9650
.9700
.9750
.9800
.9850
.9900

FIGURE 25

at atmospheric pressure (figures 16 and 19) leads to the conclusion that the surface adsorbed species must play a significant role. The behavior of the line width of the signal at g=1.957 further amplifies this (figure 22). The first and last entries in Table V and a comparison of the temperature dependence of line width under vacuum and at atmospheric pressure indicate that the surface adsorbed species play a strong role in the relaxations, but that the spin density of the sample is not effected.

The line @ g=1.96 for undoped ZnO has been resolved by other researchers into two lines at low temperature and under vacuum. These lines have been variously attributed to Zn^+, O_2^-, O^- and oxygen ion vacancies [2, 5, 15, 18, 28]. However, under no circumstances did the line @ g=1.957 for indium doped ZnO appear to be more than a single line. The suggestion that the scatter in g-value for this line is due to the relative magnitudes of two lines is not warranted, and, therefore, the change in g must be considered to be a real effect due to the dopant concentration.

The observation of two lines in ZnO by other workers led to attempts to prepare vapor grown ZnO which would be either zinc rich or oxygen rich. These samples were prepared as described earlier and their EPR spectra obtained at room temperature and atmospheric pressure. The spectra were weak showing a single line with g-values as listed in Table VII. Further attempts to resolve these lines were not made.

Table VII

Sample	H_2-O_2 Flow Ratio CFH	g-value
13A Zn Rich	0.25 : 0.15	1.9581
2B Stoichiometric	0.25 : 0.25	1.9581
4B O_2 Rich	0.25 : 0.30	1.9577
7B O_2 Rich	0.25 : 0.35	1.9581

E. CONTAMINATION

It was of interest that after outgassing one of the samples, a line in the EPR spectrum appeared which was not apparent before the treatment. The line had a narrow, intense Lorentzian line shape with a g-value near that of the free electron. Using the apparatus shown in figure 5, it was possible to bleed gasses into the sample tube while in the spectrometer cavity and then re-evacuate. With this set-up, a strip-chart recorder, and using a fast field scan over 25 gauss, it was found that this signal disappeared immediately when the pressure on the sample cavity was raised to ≈ 400 Torr with either N_2 or O_2. Re-evacuation of the sample tube (which took less than 5 seconds) immediately restored the signal to its original intensity. Based on the behavior of the signal found in this study, the line was assigned to carbon contamination from the vacuum system. This line has a g-value of 2.0028±0.0001. This assignment is substantiated by Miller et al [29] who state that under the same conditions of heat and vacuum a similar line has been observed in other

metal oxide EPR spectra. The signal was assigned to small amounts of carbon from the vacuum system which adsorbs on the oxide surface. Exposure to O_2 caused the signal to be undetectable but was restored reversibly when re-evacuated.

Another source of contamination was found to be due to Fe_3O_4 having a broad (w=2000-3000G) ferro magnetic resonance which caused some difficulty with other EPR signal base line determinations. The source of the Fe_3O_4 was some of the sample handling equipment (i.e., pellet press, furnace rod, etc.). In future work it would be well to guard against such contamination.

F. A PROPOSED MODEL FOR SPIN PAIRING

If electron pairing occurs the number of unpaired electrons observed will be determined by Fermi-Dirac statistics. The density of states profile will be determined by the energy levels of randomly positioned interacting indium ions in the lattice. It is assumed here that the density of states is a constant over the width of the donor band. Letting the number of electrons with spin up be N_+ and with spin down be N_- then in a magnetic field,

$$N_{\pm} = \frac{N}{\Delta E} \int_0^{\Delta E} \frac{d\varepsilon}{1 + e^{-\mu/kT} e^{\varepsilon/kT} e^{\mp g\beta H/2kT}} \qquad (1)$$

where ΔE is the band width, μ is determined such that $N_- + N_+ = N$ and $g\beta H$ is the energy separation of the two spin states

of a non-interacting electron in a magnetic field. Utilizing standard integrals equation (1) yields:

$$N_{\pm} = N - \frac{NkT}{\Delta E} \ln\left(1+e^{\frac{-2\mu \pm g\beta H}{2kT}} e^{\Delta E/kT}\right). \qquad (2)$$

The parameter μ is determined from equation (1).

$$\mu = \frac{\Delta E}{2} - kT \ln\left(1-e^{-\Delta E/2kT}\right) \qquad (3)$$

The number of unpaired electrons observed will be $N_- - N_+$ which from equation (2)is:

$$N_- - N_+ = \frac{N}{x} \ln\left[\frac{1+e^{x}.e^{\frac{-2\mu+g\beta H}{2kT}}}{1+e^{x}.e^{\frac{-2\mu-g\beta H}{2kT}}}\right] \qquad (4)$$

where $x = \frac{\Delta E}{kT}$.

Substituting equation (3) into equation (4) and defining $y = \frac{g\beta H}{kT}$ yields

$$N_- - N_+ = \frac{N}{x} \ln\left[\frac{1+(e^{x/2}-1)e^{y/2}}{1+(e^{x/2}-1)e^{-y/2}}\right] \qquad (5)$$

From equation (5) as $\Delta E \longrightarrow 0$ the expression simplifies to

$$N_- - N_+ = N \frac{g\beta H}{2kT} \qquad (6)$$

which would be expected for non-interacting electrons. In the upper limit where $\Delta E >> kT$ equation (5) becomes:

$$N_- - N_+ = \frac{Ng\beta H}{\Delta E} \qquad (7)$$

which is in agreement with classical theory for electrons in a band [43].

SUMMARY AND CONCLUSION

Zinc oxide can be doped with indium using the vapor transport method of crystal growth, and the doping level can be somewhat controlled by mixing the starting materials in the concentrations desired in the crystalline product. In this method the morphology of the crystals is dependent on the total gas flow rate, reducing and oxidizing gas flow ratios, temperature, and doping level.

When zinc oxide is mechanically stressed, three lines at g=2.01 appear in the EPR spectrum. This spectrum can also be induced in damaged indium doped ZnO but the relative intensities of the lines are altered and the signals are much weaker. This behavior is not understood. Observation of the three lines in ZnO indicates that the signals are due to more than one species which interact with paramagnetic centers induced in the surface of the oxide due to the stress condition.

The EPR spectrum of indium doped ZnO is a single slightly anisotropic line @ g=1.957, with line width and g-value which increases as the indium concentration is increased. In general, the g-value was independent of temperature and pressure. The line width, however, decreases with temperature with greater narrowing occurring when at atmospheric pressure than when under vacuum.

The temperature dependence of M*T for indium doped ZnO shows an increasing number of paramagnetic centers with increasing temperature, whereas M* decreased. Spin density measurements on indium doped ZnO over three decades of indium concentration did not have a one-to-one correspondence. This dependence does not have a linear correlation with the conductivity dependence on concentration of indium doped single crystals of ZnO. The observed behavior is attributed to spin pairing of the donor electrons. These observations are not consistent with the expected behavior of conduction electrons, and therefore, the electrons which give rise to the EPR signal at 1.957 in indium doped ZnO are thought to be in a shallow donor band.

APPENDIX A

The summary of g-values attributed to zinc oxide and adsorbed species on zinc oxide in this Appendix are diagrammatically displayed. The spacing of the lines is based on g for DPPH occurring at 2.0036 at a field of 3400 gauss. Each page covers a sweep width of 33.3 gauss.

g=1.95392	UV irradiated polycrystalline ZnO @ 298°K
g=1.955	In doped ZnO single crystal-conduction e^-'s
g=1.956	In doped ZnO single crystal-conduction band mobile electrons
g=1.956	ZnO powder
g=1.956	cf. 1.957
g=1.957	ZnO powder heated in air @ 900°C-measured @ 77°K attributed to oxygen vacancies
g=1.957	Conduction e^-'s in bulk ZnO. e^-'s trapped at oxygen ion vacancies
g=1.96	Doped ZnO-conduction e^-'s
g=1.96	Red ZnO @ 77°K and 300°K-stronger with UV excitation but does not shift
g=1.961	TBHP on ZnO (cf. g=1.965 these two not believed due to single species)
g=1.963	Excess Zn^+, may also be trapped e^- at O vacancies, see g=1.957. May also be e^-'s trapped at oxygen vacancies at the surface
g=1.965	TBHP on ZnO

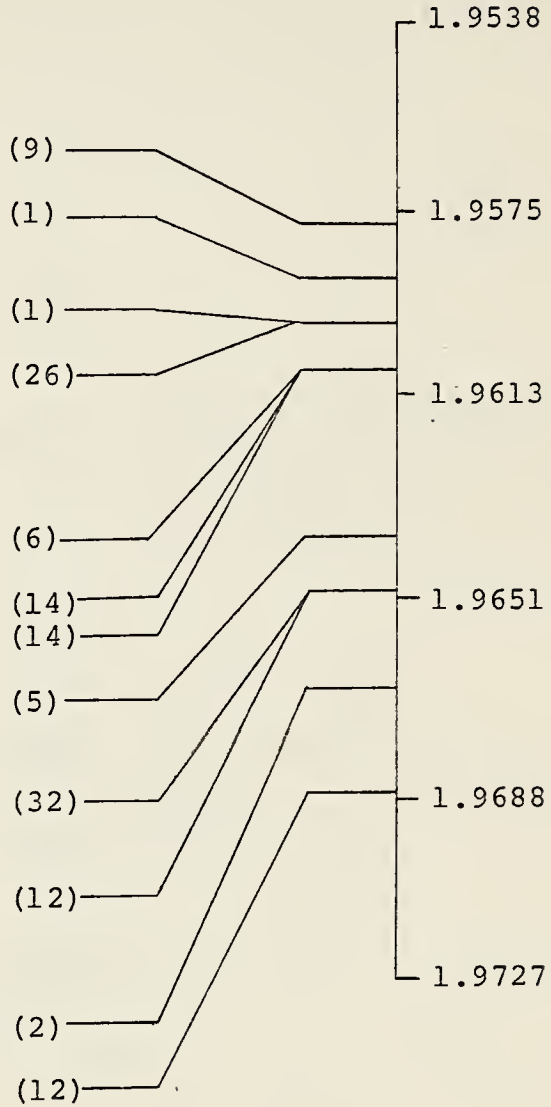

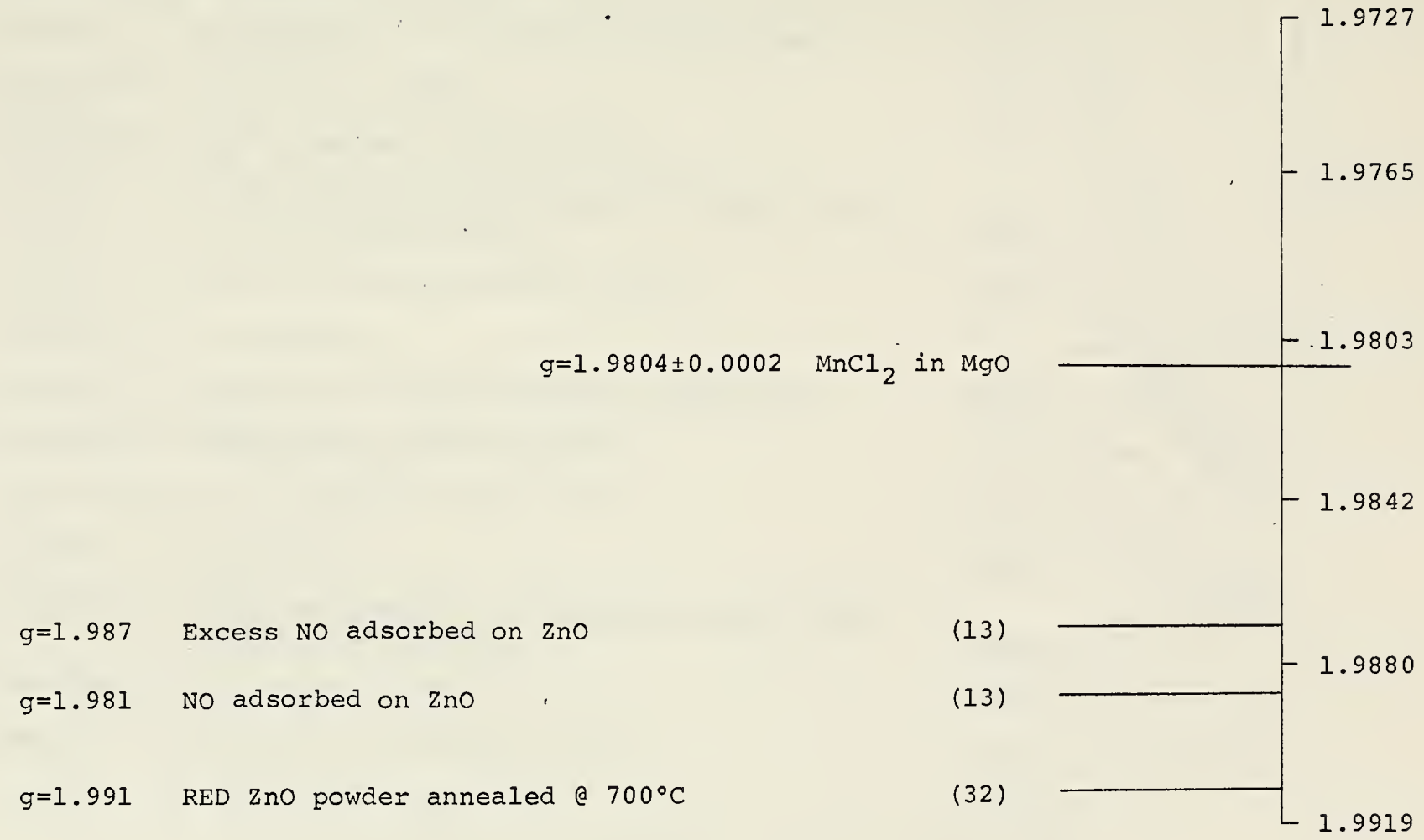
1.9727
1.9765
1.9803
g=1.9804±0.0002 $MnCl_2$ in MgO
1.9842
g=1.987 Excess NO adsorbed on ZnO (13)
1.9880
g=1.981 NO adsorbed on ZnO (13)
g=1.991 RED ZnO powder annealed @ 700°C (32)
1.9919

$g_{xx}=1.999=g_{yy}$	NO adsorbed on ZnO @ 77°K	(11)
g=2.000	NO adsorded on ZnO and excess NO on ZnO	(13)
g=2.0020	O_2^- on ZnO @ -190°C	(8)
g=2.0026	NO_2^{2-} adsorbed on ZnO @ 77°K	(11)
g=2.003	An e^- trapped on an ensemble of oxygen atoms on the surface of ZnO	(17)
g=2.003	ZnO @ 77°K-outgassed-weak signal	(13)
g=2.0033	cf. g=2.0188	
g=2.004	Milled ZnO (Disappeared upon evacuation)	(15)
g=2.0055	Mechanically pulverized ZnO	(4)
$g_{xx}=2.0057=g_{yy}$	NO_2^{2-} adsorbed on ZnO @ 77°K	(11)
g=2.006	ZnO powder	(26)
g=2.0065	Ground ZnO powder - Disappeared above 100°C remained under vacuum	(26)
g=2.0082	O_2^- on ZnO @ -190°C	(8)
g=2.009	ZnO with O_2 treatment @ 77°K	(13)
g=2.01	Mechanically damaged ZnO	(17)

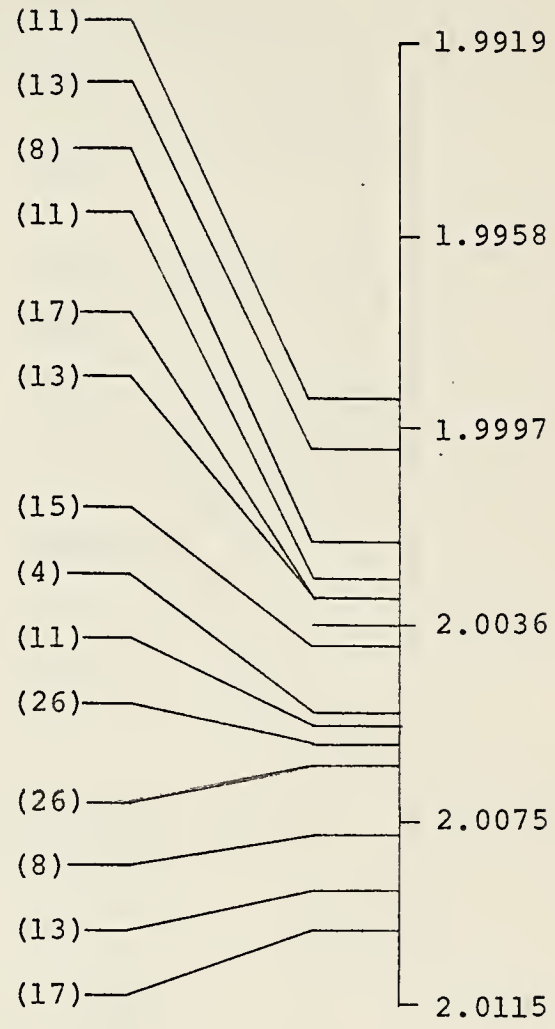

g=2.012	Polycrystalline ZnO with O_2 treatment
g=2.013	Not identified
g=2.013	Holes in acceptor levels disappeared when H_2O adsorbed; e^-'s at O_2 vacancies
g=2.0136	Milled ZnO (Disappeared upon evacuation)
g=2.015	(Not observed above -130°C) ZnO treated with NO_2 NO_2 molecules on surface
g=2.016	Excess NO adsorbed on ZnO
g=2.018	NO adsorbed on ZnO
g=2.0187	Milled ZnO (Disappeared upon evacuation)
g=2.0188) g=2.0192) g=2.0033)	Single Crystal ZnO Zn vacancies

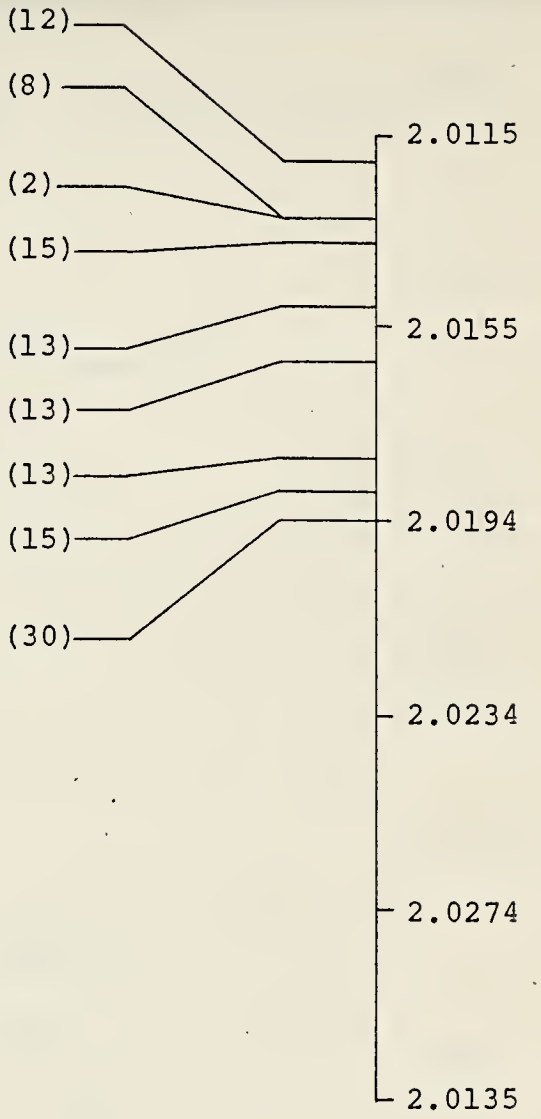

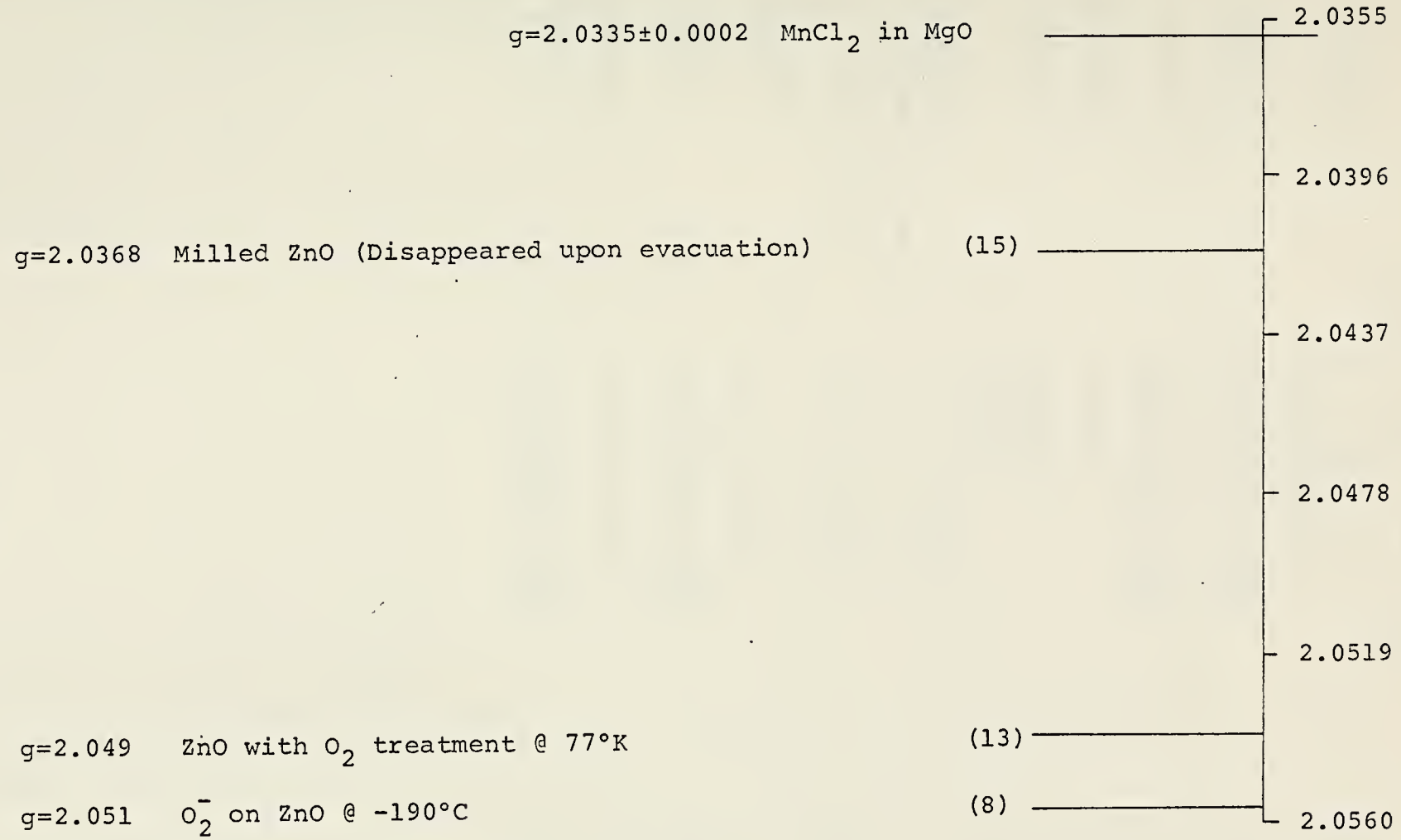
g=2.0335±0.0002 $MnCl_2$ in MgO
2.0355
2.0396
g=2.0368 Milled ZnO (Disappeared upon evacuation)
(15)
2.0437
2.0478
2.0519
g=2.049 ZnO with O_2 treatment @ 77°K
(13)
g=2.051 O_2^- on ZnO @ -190°C
(8)
2.0560

SUBSTITUTIONAL IONS IN ZnO

		Ref.
ZnO-Gd^{3+}	$g_{\parallel}=1.987\pm0.002$ $g_{\perp}=1.978\pm0.002$	33
ZnO-Co^{2+}	$g_{\parallel}=2.2500\pm0.0001$ $g_{\perp}=4.5536\pm0.0001$	34
ZnO-Fe^{3+}	$g_x=2.0056\pm0.0001$ $g_z=2.0041\pm0.0002$	35
ZnO-Fe^{3+}	$g=2.0058$	36
ZnO-I_2	$g=2.0132$ $g=2.0012$ $g=1.9639$	37
ZnO-Yb^{3+} (Substitutional)	$g_{\parallel}=1.311\pm0.001$ $g_{\perp}=4.421\pm0.001$	
(Interstitial)	$g_{\parallel}=4.812\pm0.002$ $g_{\perp}=2.390\pm0.003$	38
ZnO-V^{3+}	$g_{\parallel}=1.945\pm0.001$ $g_{\perp}=1.937\pm0.002$	39
ZnO-V^{3+}	$g_{\parallel}=1.9451\pm0.0005$ $g_{\perp}=1.9328\pm0.0005$	40
ZnO-Pb^{3+}	$g=2.013\pm0.0002$	41
ZnO-Sn^{3+}	$g_{\parallel}=1.9877\pm0.0002$ $g_{\perp}=1.9868\pm0.0001$	31

APPENDIX B

FIRST MOMENT COMPUTATION

If the EPR absorption is Lorentzian the line shape has the analytical form

$$g(\omega) = \frac{T_2}{\pi} \frac{1}{1 + T_2^2(\omega-\omega_0)^2}$$

where T_2 is the spin-spin (or transverse) relaxation and ω_0 is the center frequency (figure 24) [42]. The EPR spectrum of this absorption is recorded as the first derivative (figure 25). In general, the Lorentzian line shape has the form

$$f(x) = \frac{I}{1 + T_2^2x^2} \qquad \text{(B-1)}$$

where $x=\omega-\omega_0$ and $I=T_{2/\pi}$

The first derivative is

$$f'(x) = \frac{-2IT_2^2x}{(1+T_2^2x^2)^2} \qquad \text{(B-2)}$$

In order to find the integrated intensity of the absorption f(x) must be integrated from $-\infty$ to $+\infty$.

$$A = \int_{-\infty}^{\infty} f(x)dx \qquad \text{(B-3)}$$

This integral may be evaluated by taking the first moment of the first derivative which can be shown to be equivalent to equation (B-3).

$$A = -\int_{-\infty}^{\infty} xf'(x)dx \qquad \text{(B-4)}$$

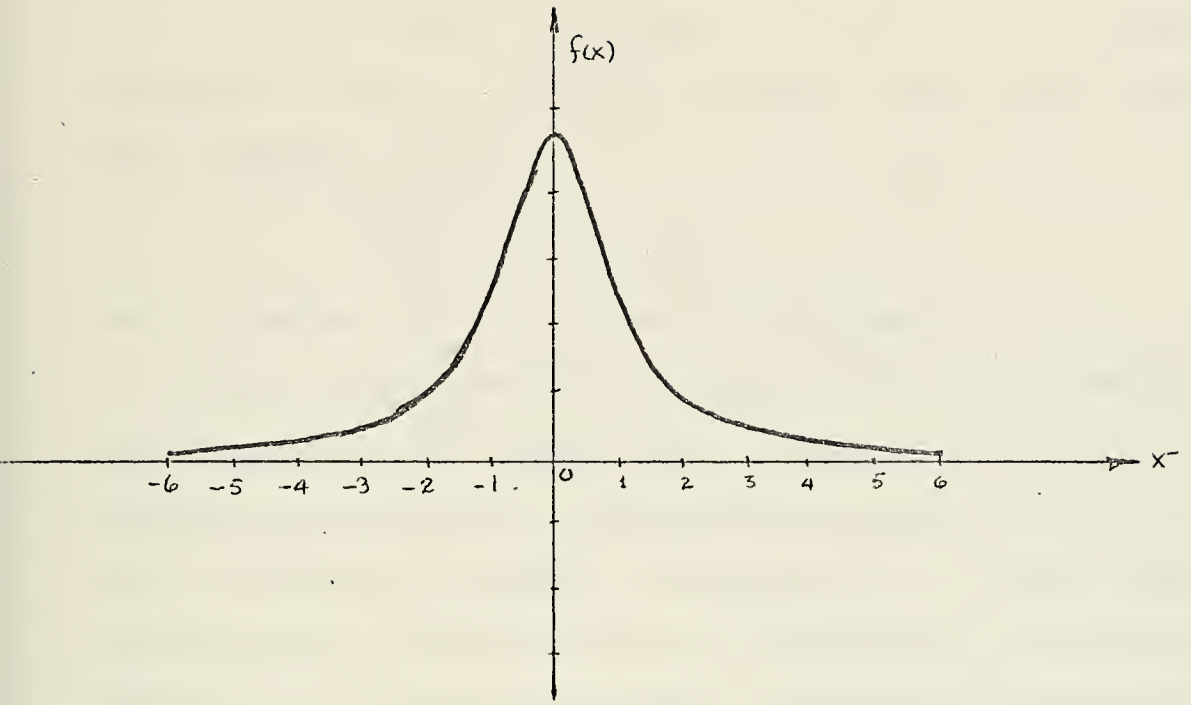

FIGURE 24

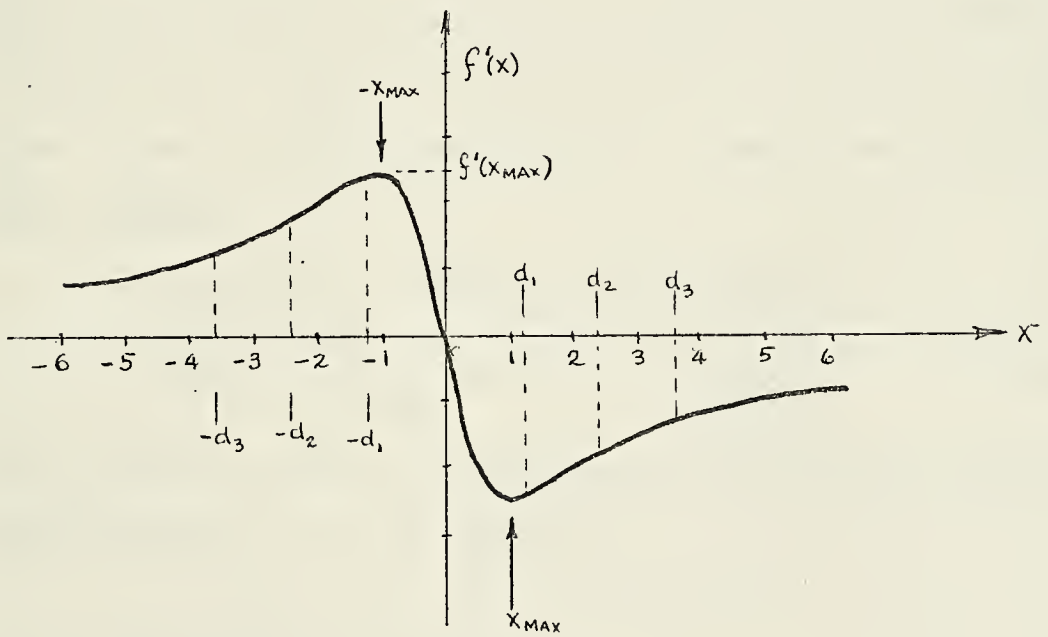

FIGURE 25

Integration by parts yields:

$$A = -xf(x)\Big|_{-\infty}^{\infty} + \int_{-\infty}^{\infty} f(x)dx \qquad \text{(B-5)}$$

Taking the limit as $x \longrightarrow \infty$ of the first part of the right hand expression yields

$$\lim_{x \longrightarrow \infty} \{xf(x)\} \longrightarrow o$$

Hence equation (B-4) is equivalent to equation (B-3).

A first moment computation using numerical methods can then be made point by point out to infinity in the plus and minus directions, and providing the procedure is carried out to completion no error should result. It would, however, be impractical to perform such an integration to the limits required. If, on the other hand, the limits of integration were chosen such that only nine or ten times the peak to peak width of the first derivative curve were included, substantial error results. A correction for this error must be made. Choosing $\pm d$ as the limits of integration equation (B-5) becomes

$$A = F(d) = -xf(x)\Big|_{-d}^{d} + \int_{-d}^{d} f(x)dx$$

$$F(d) = 2I\left[\frac{1}{T_2}\tan^{-1}T_2 d - \frac{d}{1+T_2^2 d^2}\right] \qquad \text{(B-6)}$$

When equation (B-5) is evaluated the first part of the right hand expression is zero and since

$$-\pi/2 < \tan^{-1} x < \pi/2 \text{ for } -\infty < x < \infty$$

the resulting equation is

$$A = F(\infty) = \frac{I}{T_2}\tan^{-1} T_2 x \Big|_{-\infty}^{\infty}$$

$$F(\infty) = \frac{\pi I}{T_2} \qquad \text{(B-7)}$$

The fraction of the total area under the Lorentz line shape obtained by choosing d as the limits of integration is then

$$\frac{F(d)}{F(\infty)} = \frac{1}{\pi}\left[2\tan^{-1} T_2 d - \frac{2T_2 d}{1+T_2^2 d^2}\right] \qquad \text{(B-8)}$$

From this relationship and knowing F(d) from point by point evaluation, d and T_2, F(∞) can be determined.

$$F(\infty) = \frac{F(d)}{\frac{2}{\pi}\left(\tan^{-1} T_2 d - \frac{T_2 d}{1+T_2^2 d^2}\right)} \qquad \text{(B-9)}$$

In order to find T_2 the maximum of the first derivative must be determined. Taking the second derivative, setting it equal to zero and solving for T_2 yields:

$$T_2 = \pm \frac{1}{\sqrt{3}\, x_{max}} \qquad \text{(B-10)}$$

where x_{max} can be taken off the EPR spectrum (figure 25).

Another parameter which is easily obtained from the EPR spectrum is $f'(x_{max})$ (figure 25). Evaluating the first derivative at x_{max} gives

$$f'(x_{max}) = \frac{3\sqrt{3}}{8} I T_2 \qquad \text{(B-11)}$$

Having evaluated F(d) from the EPR trace, and calculated F(∞), which is based on an estimate of T_2 a better value of T_2 can be obtained by equation (B-12)

$$\frac{f'(x_{max})}{F(\infty)} = \frac{\frac{3\sqrt{3}}{8}(IT_2)}{\pi/T_2 (I)} .$$

Solving for T_2 yields

$$T_2 = \left[\frac{\pi f'(x_{max})}{3\sqrt{3}\, F(\infty)}\right]^{\frac{1}{2}} \qquad \text{(B-12)}$$

Using the value of T_2 derived from equation (B-12) a new value of $F(\infty)$ from equation (B-9) can be calculated and then a better value of T_2 and so on until a self-consistent value of T_2 is obtained.

In the above discussion it was assumed that the absorption was Lorentzian. Therefore, regardless of the limits of integration, d, for which F(d) is obtained an accurate value of $F(\infty)$ is possible. For example, if in figure 25 $F(d_1)$ is evaluated and subsequently $F(\infty)$, the same result must obtain if $F(d_2)$ is evaluated and then $F(\infty)$ calculated. In addition, the line width parameter T_2 must be the same in both cases if the absorption is truly Lorentzian. Conversely, if there is significant deviation in T_2 from $F(d_1)$ to $F(d_2)$, etc., T_2 will be a measure of the deviation of the experimental EPR line from the truly Lorentz line shape.

An example using this method to find the integrated intensity of the EPR spectrum of $CuSO_4 \cdot 5H_2O$ gave values for $F(\infty)$ which varied 1.3 units^2 in 120 or about one percent, when integration limits from one to eight units were used (figure 26). The corresponding values of T_2 are plotted in figure 27. The consistent value of $F(\infty)$ and small deviation

FIGURE 26

FIGURE 27

in T_2 are evidence of a Lorentz line shape. In general, consistent results are obtained when the first integration limit, d_i, used to evaluate $F(\infty)$ is such that at least one half line width is exceeded (i.e., $|\Sigma_i d_i| > |x_{max}|$) and, since the size of d is arbitrary it is a good rule when evaluating the first moment to choose increments in d such that at least one or two points of $f'(x)$ are used before $f'(x_{max})$ is reached.

For a symmetric line shape, exactly half of the area is one one side of the center. It should be possible, if the base line is accurately known, to evaluate F(d) from 0 to d and double the value to shorten the procedure. But the stipulation of an accurate base line is in practice not always easy to meet, particularly if there is even a small overlap from some other line in the EPR spectrum. To reduce this error a point by point first moment should be evaluated on both sides of the first derivative curve and added.

APPENDIX C

EPR spectrum of In_2O_3

g=1.8822±0.0008

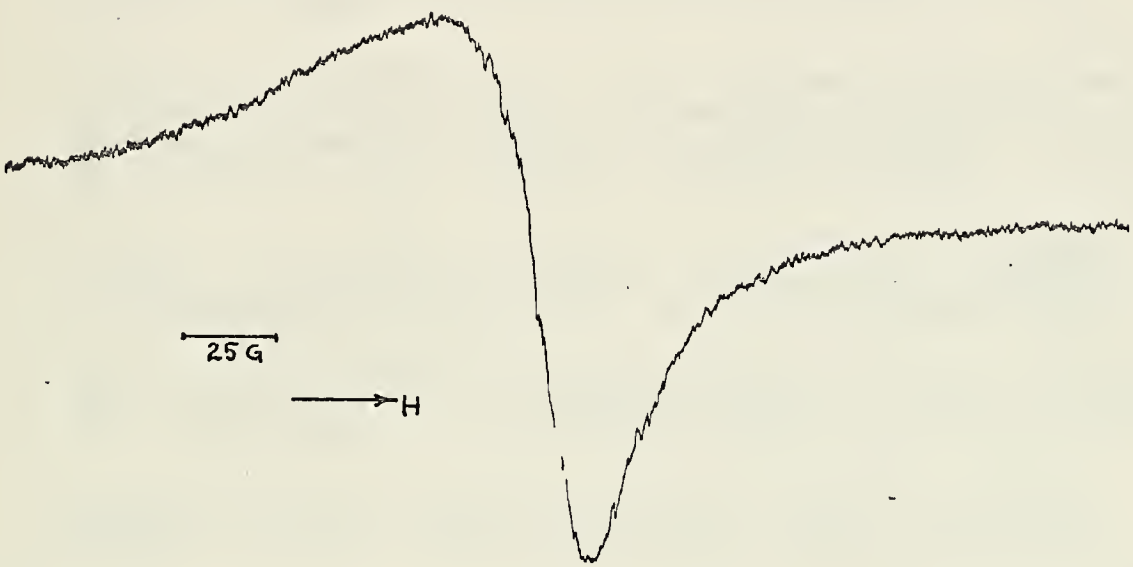

BIBLIOGRAPHY

1. Müller, K. A. and Schneider, J., "Conduction Electron Spin Resonance in Group II-VI Semiconductors and Phosphors", Physics Letters (Netherlands), v. 4-5, p. 288-291, 1 May 1963.

2. Setaka, M., Fujieda, S. and Kwan, T., "Electron Spin Resonance of Oxidized ZnO at -195°C", Bulletin of the Chemical Society of Japan, v. 43-8, p. 2377-2380, 1970.

3. Thomas, D. G., "The Diffusion and Precipitation of Indium in Zinc Oxide", J. Phys. Chem. Solids, v. 9, p. 31-42, 1958.

4. Walters, G. K. and Estle, T. L., "Paramagnetic Resonance of Defects Introduces Near the Surface of Solids by Mechanical Damage", Journal of Applied Physics, v. 32-10, p. 1854-1859, October 1961.

5. Kokes, R. J., "The Influence of Chemisorption of Oxygen on the Electron Spin Resonance of Zinc Oxide", Journal of Physical Chemistry, v. 66, p. 99-103, January 1962.

6. Kasai, P. H., "Electron Spin Resonance Studies of Donors and Acceptors in ZnO", Physical Review, v. 130-3, p. 989-995, 1 May 1963.

7. Rauber, A. and Schneider, J., "Localized $^2S_{1/2}$-State Centres in ZnS", Phys. Stat. Sol., v. 18, p. 125-132, 1966.

8. Lunsford, J. H. and Jayne, J. P., "Electron Paramagnetic Resonance of Oxygen on ZnO and Ultraviolet-Irradiated MgO", Journal of Chemical Physics, v. 44-1, p. 1487-1492, 15 February 1966.

9. Lal, R. B. and Arnett, G. M., "Electron Paramagnetic Resonance of Photosensitive Donors in ZnO", J. Phys. Soc. Japan, v. 21, p. 2734-2735, 1966.

10. Sancier, K. M., "ESR Evidence of CO Oxidation by More Than One Oxygen Species Sorbed on ZnO", Journal of Catalysis, v. 9, p. 331-335, 1967.

11. Lunsford, J. H., "Surface Interactions of Zinc Oxide and Zinc Sulphide with Nitric Oxide", Journal of Physical Chemistry, v. 72-6, p. 2141-2144, June 1968.

12. Codell, M., Gisser, H., Weisberg, J. and Iyengar, R. D., "Electron Spin Resonance Study of Hydroperoxide on Zinc Oxide", Journal of Physical Chemistry, v. 72-7, p. 2460-2464, July 1968.

13. Iyengar, R. D., Subba Rao, V. V. and Zettlemoyer, A. C., "ESR Studies of the Interaction of O_2, NO_2, N_2O, NO and Cl_2 with Zinc Oxide", Surface Science, v. 13, p. 261-262, 1969.

14. Setaka, M., Sancier, K. M. and Kwan, T., "Electron Spin Resonance Investigation of Electrical Conductivity Parameters of Zinc Oxide During Surface Reactions", Journal of Catalysis, v. 16, p. 44-52, 1970.

15. Sancier, K. M., "ESR Investigation of Photodamage to Zinc Oxide Powders", Surface Science, v. 21, p. 1-11, 1970.

16. Born, G. K., Hofstaetter, A. B., Scharmann, A. O., Arnett, G. M., Kroes, R. L. and Wegner, U. E., "EPR Investigations on X-Ray and Photo-Induced Processes in ZnO Coating Material", Phys. Stat. Sol., v. A4, p. 675-684, 1971.

17. Mookherji, T., "Electron Spin Resonance of Ultraviolet Radiation Induced Defects in ZnO Thermal Control Coating Pigment", Phys. Stat. Sol., v. A13, p. 293-301, 1972.

18. Gerasimova, G. F. and Keier, N. P., "Dependence of the Character of the Defects in Zinc Oxide on the Method of Preparation and Conditions of Treatment", Kinetics and Catalysis, v. 12-5, p. 1039-1042, 1971.

19. Tanaka, K. and Blyholder, G., "Adsorbed Oxygen Species on Zinc Oxide in the Dark and Under Illumination", The Journal of Physical Chemistry, v. 76-22, p. 3184-3187, 1972.

20. Sancier, K. M., "Temperature Dependence of the Electron Spin Resonance Spectra of Zinc Oxide Powder", The Journal of Physical Chemistry, v. 76-18, p. 2527-2529, 1972.

21. Scharowsky, E., "Optische und Elektrische Eigenschaften von ZnO-Einkristallen mit Zn-Uberschuss", Zietschrift für Physik, v. 135, p. 318-330, 1953.

22. Dodson, E. M. and Savage, J. A., "Vapour Growth of Single-Crystal Zinc Oxide", Journal of Material Science, v. 3, p. 19-25, 1968.

23. Nielson, K. F., "Growth of ZnO Single Crystals by the Vapor Phase Reaction Method", Journal of Crystal Growth, v. 3, 4, p. 141-145, 1968.

24. Bogner, G. and Mollwo, E., "Uber Die Herstellung Von Zinkoxydeinkristallen Mit Definierten Zusaten", J. Phys. Chem. Solids, v. 6, p. 136-143, 1958.

25. Kasper, H., Uber die Lichtabsorption von Halbleitenden Phasen im System ZnO-In_2O_3", Z. Anorg. Allg. Chem., v. 364, p. 215-225, 1969.

26. Golubev, V. B. and Evdokimov, V. B., "Electron Paramagnetic Resonance in Zinc Oxides Subjected to Mechanical Treatment", Russian Journal of Physical Chemistry, v. 38-2, p. 252-253, February 1964.

27. Dyson, F. J., "Electron Spin Resonance Absorption in Metals, II. Theory of Electron Diffusion and the Skin Effect", Physical Review, v. 98-2, p. 349-359, 15 April 1955.

28. Alger, R. S., Electron Paramagnetic Resonance: Techniques and Applications, p. 308ff, Interscience Publishers, 1968.

29. Miller, D. J. and Haneman, D., "Carbon EPR Signal From Vacuum Heated Surfaces", Surface Science, v. 24, p. 639-642, 1971.

30. Taylor, A. L., Filipovich, G. and Lindeberg, G. K., "Electron Paramagnetic Resonance Associated with Zn Vacancies in Neutron Irradiated ZnO", Solid State Communications, v. 8-17, p. 1359-1361, 1970.

31. Hausmann, A. and Schrieber, P., "A Paramagnetic Defect in ZnO:Sn with $(5s)^1$ Configuration", Z. Physik, v. 245, p. 184-190, 1971.

32. Larach, S. and Turkevich, J., "Characterization of Red Zinc Oxide by Electron Paramagnetic Resonance", J. Phys. Chem. Solids, v. 29, p. 1519-1522, 1968.

33. Hausmann, A., "Paramagnetic Resonance of Gd^{3+} in ZnO", Solid State Communications, v. 7-8, p. 579-583, 1969.

34. Hausmann, A., "Electron Spin Resonance of ZnO:Co^{++} Single Crystals", Phys. Stat. Sol., v. 31, p. K131-K133, 1969.

35. Hausmann, A., "Anisotropy of the g Tensor of Fe^{3+} in Zinc Oxide", Journal of the Physical Society of Japan, v. 26-1, p. 91-92, January 1969.

36. Campbell, I. D. and Cope, J. O., "A Note on the Splitting of the ($\frac{1}{2} \longleftrightarrow -\frac{1}{2}$) Line in the ESR Spectrum of Fe^{3+} in ZnO", Solid State Communications, v. 8-1, p. 45-47, 1970.

37. Larach, S. and Turkevich, J., "Iodine Effect on Electron Paramagnetic Resonance of Zinc Oxide", Surface Science, v. 20, p. 192-194, 1970.

38. Schreiber, P. and Hausmann, A., "ESR Studies of Yb^{3+} Impurities in Zinc Oxide", Solid State Communications, v. 8-14, p. 1103-1106, 1970.

39. Hausmann, A. and Blaschke, R., "ESR of V^{3+} in Zinc Oxide Single Crystals", Z. Physik, v. 230, p. 255-264, 1970.

40. Filipovich, G., Taylor, A. L. and Coffman, R. E., "Electron Paramagnetic Resonance of V^{3+} Ions In Zinc Oxide", Physical Review B, v. 1-5, p. 1986-1994, 1 March 1971.

41. Born, G., Hofstaetter, A. and Scharmann, A., "EPR of Pb^{3+} in ZnO", Z. Physik, v. 240, p. 163-167, 1970.

42. Carrington, A. and McLachlan, An. D., Introduction to Magnetic Resonance, p. 9 and 182, Harper & Row Publishers, 1967.

43. Kittel, C., Introduction to Solid State Physics, 4th ed., p. 249, John Wiley & Sons, Inc. 1971.

INITIAL DISTRIBUTION LIST

		No. Copies
1.	Defense Documentation Center Cameron Station Alexandria, Virginia 22314	2
2.	Library, Code 0212 Naval Postgraduate School Monterey, California 93940	2
3.	Professor W. M. Tolles, Code 61T1 Department of Physics and Chemistry Naval Postgraduate School Monterey, California 93940	1
4.	Lcdr Coenraad van der Schroeff, USN 22306 Capote Drive Salinas, California 93901	1
5.	Dr.William S. McEwan, Code 604 Naval Weapons Center China Lake, California 93555	1

DOCUMENT CONTROL DATA - R & D

(Security classification of title, body of abstract and indexing annotation must be entered when the overall report is classified)

1. ORIGINATING ACTIVITY (Corporate author)

Naval Postgraduate School
Monterey, California 93940

2a. REPORT SECURITY CLASSIFICATION

Unclassified

2b. GROUP

3 REPORT TITLE

An Electron Paramagnetic Resonance Study of Indium Doped Zinc Oxide

4. DESCRIPTIVE NOTES (Type of report and inclusive dates)

Master's Thesis; June 1973

5. AUTHOR(S) (First name, middle initial, last name)

Coenraad van der Schroeff

6. REPORT DATE	7a. TOTAL NO. OF PAGES	7b. NO. OF REFS
June 1973	97	43

8a. CONTRACT OR GRANT NO.	9a. ORIGINATOR'S REPORT NUMBER(S)
b. PROJECT NO.	
c.	9b. OTHER REPORT NO(S) (Any other numbers that may be assigned this report)
d.	

10. DISTRIBUTION STATEMENT

Approved for public release; distribution unlimited

11. SUPPLEMENTARY NOTES	12. SPONSORING MILITARY ACTIVITY
	Naval Postgraduate School Monterey, California 93940

13. ABSTRACT

Samples of zinc oxide doped with indium have been prepared using the vapor transport method. Concentration of dopant is controlled by appropriate mixing of the oxides of indium and zinc.

When ZnO is mechanically damaged, three lines in the EPR spectrum with g-values at 2.0052, 2.0136, 2.0184 are induced. These are attributed to the interaction of adsorbed species and induced paramagnetic centers in the crystal. The relative intensity of the lines is affected by indium doping.

Spin density measurements using first moment calculations (M*) on ZnO-In did not show a linear correlation with concentration. This is attributed to spin pairing of the electrons. The g-value for ZnO-In varied depending on concentration from 1.9563 to 1.9591, and was found to be independent of temperature and pressure.

Based on the behavior of M*T and M* for In doped ZnO the electrons giving rise to the EPR spectrum were thought to be in a shallow donor band.

KEY WORDS	LINK A		LINK B		LINK C	
	ROLE	WT	ROLE	WT	ROLE	WT
Zinc Oxide						
Indium doped zinc oxide						
Electron Paramagnetic Resonance						
mechanically damaged zinc oxide						
vapor transport growth of indium doped zinc oxide						
Atomic Absorption indium analysis						

Thesis
V162
c.1
145217
Van der Schroeff
An electron paramagnetic resonance study of indium doped zinc oxide.